

Loop induced Higgs and Z boson couplings to Neutralinos and implications for collider and Dark Matter searches

A. DJOUADI¹, M. DREES², P. FILEVIEZ PEREZ³ and M. MÜHLEITNER¹

¹*Laboratoire de Physique Mathématique et Théorique, UMR5825-CNRS,
Université de Montpellier II, F-34095 Montpellier Cedex 5, France.*

²*Physik Department, Technische Universität München,
James Franck Strasse, D-85748 Garching, Germany.*

³*Max-Planck Institut für Physik (Werner-Heisenberg Institut)
Föhringer Ring 6, 80805 München, Germany.*

Abstract

We calculate the one-loop induced couplings of two gaugino-like neutralinos to the Z and Higgs bosons in the Minimal Supersymmetric Standard Model. These couplings, which vanish at the tree level, can be generated through loops involving fermions and sfermions. We show that, while the neutralino contribution to the invisible Z boson decay width remains small, the loop induced couplings to the lightest Higgs boson might be sufficiently large to yield a rate of invisible decays of this Higgs boson that should be detectable at future e^+e^- colliders. We also study the implications of these couplings for direct searches of Dark Matter and show that they can modify appreciably the neutralino-nucleon elastic cross section for some parameter range.

1 Introduction

The Minimal Supersymmetric Standard Model (MSSM) [1] is at the moment considered to be the most plausible extension of the Standard Model (SM). Out of the plethora of new particles contained in this model the lightest neutralino $\tilde{\chi}_1^0$ plays a special role. It is often the lightest of all superparticles (LSP), which is absolutely stable if R-parity is conserved. This means that neutralino LSPs produced at colliders will be invisible, leading to the famous “missing [transverse] momentum” signatures for the production of superparticles. In particular, a final state consisting of two LSPs only would be entirely invisible, so that $\tilde{\chi}_1^0\tilde{\chi}_1^0$ final states can contribute to the invisible width of the Z or neutral Higgs bosons. Moreover, if the LSP is stable, we expect some relic LSPs from the Big Bang era to still exist today, in addition to the well-known relic neutrinos and (microwave) photons. In fact, it was realized almost twenty years ago that $\tilde{\chi}_1^0$ is a good (cold) Dark Matter (DM) candidate [2]. The LSP–nucleon scattering cross section, which determines the size of the expected signal in direct DM detection experiments [3], depends on the size of the LSP couplings to the Z and Higgs bosons; these couplings can also play a role in the calculation of the $\tilde{\chi}_1^0$ relic density. A precise knowledge of these couplings is therefore important for both collider phenomenology and cosmology.

The lightest neutralino $\tilde{\chi}_1^0$ couples to the Z boson and to the MSSM Higgs bosons only if it has a non-vanishing higgsino component. On the other hand, most models predict $\tilde{\chi}_1^0$ to be dominantly a gaugino, in particular, a bino- or photino-like state. Moreover, an LSP with dominant higgsino component has a thermal relic density of the required magnitude only if its mass is in the TeV range, beyond the reach of near-future colliders and also beyond the range of masses that is usually considered to be natural. In contrast, a bino-like LSP is a good thermal DM candidate for masses in the 100 GeV range; masses in this range are more natural, and can be probed at present and near-future colliders. Since these gaugino-like states have suppressed tree-level couplings to gauge and Higgs bosons, loop contributions to these couplings might be significant.

In this paper we compute one-loop corrections to the neutralino couplings to the Z and Higgs bosons, where we only consider contributions with fermions and sfermions inside the loop [the other possible contributions, involving charginos, neutralinos and Higgs or gauge bosons, vanish in the bino-like limit for the $\tilde{\chi}_1^0$]. Our analytical results for these corrections, for arbitrary momenta and general $\tilde{f}_L - \tilde{f}_R$ mixing¹, are given in Sec. 2. In Sec. 3 we apply these results to compute the loop-corrected invisible branching ratios of Z and Higgs bosons, and in Sec. 4 we study the loop-corrected LSP–nucleon scattering rate and relic density.

For the neutralino couplings to Higgs and gauge bosons, we found in all cases corrections of up to a factor of two for reasonable values of the input parameters. The contribution of bino-like LSPs to the invisible decay width of the lightest MSSM Higgs boson might be measurable at future high-energy and high-luminosity e^+e^- colliders, while the contribution to the invisible decay width of the Z boson remains several orders of magnitude below the

¹Loop corrections to the Z exchange contribution to the bino annihilation cross section have previously been computed in [4]. However, in this earlier paper $\tilde{f}_L - \tilde{f}_R$ mixing has been ignored, and analytical results are only given for vanishing LSP three-momenta. Our numerical results agree qualitatively with theirs.

present bound. On the other hand, the loop corrections can modify appreciably the LSP–nucleon scattering cross section in some MSSM parameter range.

2 Neutralino couplings to Higgs and Z Bosons

2.1 Tree-level couplings

At the tree level, the couplings of the neutralinos $\tilde{\chi}_i^0$ to the Z boson are given by the vertex² [5]:

$$\Gamma_\mu^0(Z\tilde{\chi}_i^0\tilde{\chi}_j^0) = i\frac{g}{2c_W} \gamma_\mu \gamma_5 [N_{i3}N_{j3} - N_{i4}N_{j4}] \equiv ig_{Z\tilde{\chi}_i^0\tilde{\chi}_j^0}^0 \gamma_\mu \gamma_5, \quad (1)$$

while the neutralino couplings to the neutral CP–even Higgs bosons $\phi = h, H$ and to the CP–odd boson A read [6, 7]:

$$\Gamma^0(\phi\tilde{\chi}_i^0\tilde{\chi}_j^0) = i\frac{g}{2} [(N_{i2} - \tan\theta_W N_{i1})(d_\phi N_{j3} + e_\phi N_{j4}) + i \leftrightarrow j] \equiv ig_{\phi\tilde{\chi}_i^0\tilde{\chi}_j^0}^0; \quad (2)$$

$$\Gamma^0(A\tilde{\chi}_i^0\tilde{\chi}_j^0) = \frac{g}{2} [(N_{i2} - \tan\theta_W N_{i1})(d_A N_{j3} + e_A N_{j4}) + i \leftrightarrow j] \gamma_5 \equiv g_{A\tilde{\chi}_i^0\tilde{\chi}_j^0}^0 \gamma_5. \quad (3)$$

Here, $g = e/s_W$ is the SU(2) gauge coupling with $s_W^2 = 1 - c_W^2 \equiv \sin^2\theta_W$. The quantities d_Φ, e_Φ ($\Phi = h, H, A$) are determined by the ratio $\tan\beta$ of the vacuum expectation values of the two doublet Higgs fields which are needed to break the electroweak symmetry in the MSSM, and the mixing angle α in the CP–even neutral Higgs sector:

$$\begin{aligned} d_H &= -\cos\alpha, \quad d_h = \sin\alpha, \quad d_A = \sin\beta, \\ e_H &= \sin\alpha, \quad e_h = \cos\alpha, \quad e_A = -\cos\beta. \end{aligned} \quad (4)$$

N is the matrix which diagonalizes the four dimensional neutralino mass matrix:

$$\mathcal{M}_N = \begin{bmatrix} M_1 & 0 & -m_Z s_W c_\beta & m_Z s_W s_\beta \\ 0 & M_2 & m_Z c_W c_\beta & -m_Z c_W s_\beta \\ -m_Z s_W c_\beta & m_Z c_W c_\beta & 0 & -\mu \\ m_Z s_W s_\beta & -m_Z c_W s_\beta & -\mu & 0 \end{bmatrix}, \quad (5)$$

where M_1 and M_2 are the SUSY breaking masses for the $U(1)_Y$ and $SU(2)_L$ gauginos, μ is the higgsino mass parameter, and $s_\beta \equiv \sin\beta$, etc. This matrix can be diagonalized analytically [8], but the expressions of the neutralino masses and the N_{ij} matrix elements are rather involved. However, if the entries in the off–diagonal 2×2 submatrices in eq. (5) are small compared to (differences of) the diagonal entries, one can expand the eigenvalues in powers

²We assume that all soft breaking parameters as well as μ are real, i.e. conserve CP. We can then work with a real, orthogonal neutralino mixing matrix N if we allow the eigenvalues $m_{\tilde{\chi}_i^0}$ to be negative. Note also that the vertex factors Γ given in the text are $2i$ times the coefficients of the relevant terms in the interaction Lagrangian.

of m_Z [9, 10]:

$$\begin{aligned}
m_{\tilde{\chi}_1^0} &\simeq M_1 - \frac{m_Z^2}{\mu^2 - M_1^2} (M_1 + \mu s_{2\beta}) s_W^2; \\
m_{\tilde{\chi}_2^0} &\simeq M_2 - \frac{m_Z^2}{\mu^2 - M_2^2} (M_2 + \mu s_{2\beta}) c_W^2; \\
m_{\tilde{\chi}_3^0} &\simeq -\mu - \frac{m_Z^2(1 - s_{2\beta})}{2} \left(\frac{s_W^2}{\mu + M_1} + \frac{c_W^2}{\mu + M_2} \right); \\
m_{\tilde{\chi}_4^0} &\simeq \mu + \frac{m_Z^2(1 + s_{2\beta})}{2} \left(\frac{s_W^2}{\mu - M_1} + \frac{c_W^2}{\mu - M_2} \right).
\end{aligned} \tag{6}$$

In this analysis, we are interested in the situation $|\mu| > M_1, M_2$ and $\mu^2 \gg m_Z^2$. In this case the lighter two neutralinos will be gaugino-like. If $|M_1| < |M_2|$, which is the case if gaugino masses unify at the same scale where the gauge couplings appear to meet [11], the lightest state will be bino-like, and the next-to-lightest state will be wino-like. The two heaviest states will be dominated by their higgsino components.³ The eigenvectors of the mass matrix (5) can also be expanded in powers of m_Z . We find for the bino-like state [9, 10]:

$$\begin{aligned}
N_{11} &= \left[1 + (N_{12}/N_{11})^2 + (N_{13}/N_{11})^2 + (N_{14}/N_{11})^2 \right]^{-1/2}; \\
\frac{N_{12}}{N_{11}} &= \frac{m_Z^2 s_W c_W}{\mu^2 - M_1^2} \frac{s_{2\beta} \mu + M_1}{M_1 - M_2} + \mathcal{O}(m_Z^3); \\
\frac{N_{13}}{N_{11}} &= m_Z s_W \frac{s_{\beta} \mu + c_{\beta} M_1}{\mu^2 - M_1^2} + \mathcal{O}(m_Z^2); \\
\frac{N_{14}}{N_{11}} &= -m_Z s_W \frac{c_{\beta} \mu + s_{\beta} M_1}{\mu^2 - M_1^2} + \mathcal{O}(m_Z^2).
\end{aligned} \tag{7}$$

The corresponding expressions for the wino-like state read:

$$\begin{aligned}
N_{22} &= \left[1 + (N_{21}/N_{22})^2 + (N_{23}/N_{22})^2 + (N_{24}/N_{22})^2 \right]^{-1/2}; \\
\frac{N_{21}}{N_{22}} &= \frac{m_Z^2 s_W c_W}{\mu^2 - M_2^2} \frac{s_{2\beta} \mu + M_2}{M_2 - M_1} + \mathcal{O}(m_Z^3); \\
\frac{N_{23}}{N_{22}} &= -m_Z c_W \frac{s_{\beta} \mu + c_{\beta} M_2}{\mu^2 - M_2^2} + \mathcal{O}(m_Z^2); \\
\frac{N_{24}}{N_{22}} &= m_Z c_W \frac{c_{\beta} \mu + s_{\beta} M_2}{\mu^2 - M_2^2} + \mathcal{O}(m_Z^2).
\end{aligned} \tag{8}$$

Note that the higgsino components of the gaugino-like states start at $\mathcal{O}(m_Z)$, whereas the masses of these states deviate from their $|\mu| \rightarrow \infty$ limit (M_1 and M_2) only at $\mathcal{O}(m_Z^2)$.

Inserting eqs. (7) into eq. (1) one sees that the coupling of the LSP neutralinos to the Z boson only occurs at order m_Z^2 , while eqs. (2) and (3) show that the LSP couplings to the

³Loop corrections can significantly change the mass splitting between the two higgsino-like states [12, 13].

Higgs bosons $\Phi = h, H, A$ already receive contributions at $\mathcal{O}(m_Z)$:

$$\begin{aligned} g^0(Z\tilde{\chi}_1^0\tilde{\chi}_1^0) &\sim N_{13}^2 - N_{14}^2 \sim -s_W^2 c_{2\beta} \frac{m_Z^2}{\mu^2 - M_1^2}; \\ g^0(\Phi\tilde{\chi}_1^0\tilde{\chi}_1^0) &\sim d_\Phi N_{13} + e_\Phi N_{14} \\ &\sim s_W m_Z \left[\frac{(d_\Phi s_\beta - e_\Phi c_\beta)\mu}{\mu^2 - M_1^2} + \frac{(d_\Phi c_\beta - e_\Phi s_\beta)M_1}{\mu^2 - M_1^2} \right], \end{aligned} \quad (9)$$

Similar expressions can be given for the couplings of the wino-like state. This suppression of the tree-level couplings follows from the fact that, in the neutralino sector, the Z only couples to two higgsino current eigenstates while a Higgs boson couples to one higgsino and one gaugino current eigenstate, together with the fact that mixing between current eigenstates is suppressed if $|\mu| \gg m_Z$. Both kinds of couplings thus *vanish* as $|\mu| \rightarrow \infty$.

The situation in the chargino sector is somewhat similar to what has been discussed so far. The diagonalization of the chargino mass matrix

$$\mathcal{M}_C = \begin{bmatrix} M_2 & \sqrt{2}m_W s_\beta \\ \sqrt{2}m_W c_\beta & \mu \end{bmatrix} \quad (10)$$

leads, when expanded in powers of m_W , to the two chargino masses:

$$m_{\tilde{\chi}_1^\pm} \simeq M_2 - \frac{m_W^2}{\mu^2 - M_2^2} (M_2 + \mu s_{2\beta}) \simeq m_{\tilde{\chi}_2^0}, \quad m_{\tilde{\chi}_2^\pm} \simeq \mu + \frac{m_W^2}{\mu^2 - M_2^2} (M_2 s_{2\beta} + \mu), \quad (11)$$

so that for $|\mu| \rightarrow \infty$, the lightest chargino corresponds to a pure wino state while the heavier chargino corresponds to a pure higgsino state. The couplings of the neutral Higgs bosons to chargino pairs $g^0(\Phi\tilde{\chi}_i^\pm\tilde{\chi}_i^\mp)$ are suppressed in this limit, and only the couplings $g^0(\Phi\tilde{\chi}_1^\pm\tilde{\chi}_2^\mp)$ survive. Moreover, neither the W nor the charged Higgs bosons couple the LSP to the lighter chargino in this limit, $g^0(H^\pm\tilde{\chi}_1^0\tilde{\chi}_1^\mp) \sim \mathcal{O}(m_W/\mu)$, $g^0(W^\pm\tilde{\chi}_1^0\tilde{\chi}_1^\mp) \sim \mathcal{O}(m_W^2/\mu^2)$.

However, the Z boson does have full-strength couplings to pairs of charginos $\tilde{\chi}_i^\pm\tilde{\chi}_i^\mp$, and LEP2 limits imply that even the lighter chargino is too heavy to be produced in the decay of the lighter neutral Higgs boson h . Moreover, the heavy Higgs bosons can always undergo unsuppressed decays into at least some SM fermions; in fact, decays involving b -quarks are usually enhanced at large $\tan\beta$. We therefore do not expect heavy Higgs decays into modes that vanish for $|\mu| \rightarrow \infty$ to be significant even after loop corrections have been applied. For these reasons we will not discuss the chargino sector any further in this paper.

2.2 One-loop induced couplings

At the one-loop level, the couplings of the lightest neutralinos to the Z and Higgs bosons can be generated, in principle, by diagrams with the exchange of either sfermions and fermions, or of charginos or neutralinos together with gauge or Higgs bosons, in the loop. However, the latter class of diagrams can contribute to the couplings of Higgs bosons to neutralinos only if one of the particles in the loop is a higgsino. Similarly, these gauge-Higgs loops will contribute to the coupling of bino-like LSPs to the Z boson only if at least one particle in

the loop is a higgsino-like state. These loop contributions will thus be suppressed by inverse powers of $|\mu|$, in addition to the usual loop suppression factor. We therefore do not expect them to be able to compete with the tree-level couplings that exist for finite $|\mu|$, see eq. (9).⁴

We thus only consider diagrams with fermions and sfermions in the loop, as shown in Fig. 1. In the case of the $Z\tilde{\chi}_1^0\tilde{\chi}_1^0$ coupling, all three generations of matter particles will be involved since they have full gauge coupling strength. In the case of the $\Phi\tilde{\chi}_1^0\tilde{\chi}_1^0$ couplings, only the third generation (s)particles, which have large Yukawa couplings, can give significant contributions to the amplitudes. Note that in the bino limit there is no wave function renormalization to perform, since the tree-level couplings are zero. Off-diagonal wave function renormalization diagrams could convert one of the gaugino-like neutralinos into a higgsino-like state, but this kind of contribution is again suppressed by $1/|\mu|$, and can thus not compete with the tree-level coupling. In case of the Z coupling, both external gauginos would have to be converted to higgsino-like states, which is obviously only possible at the two-loop level.

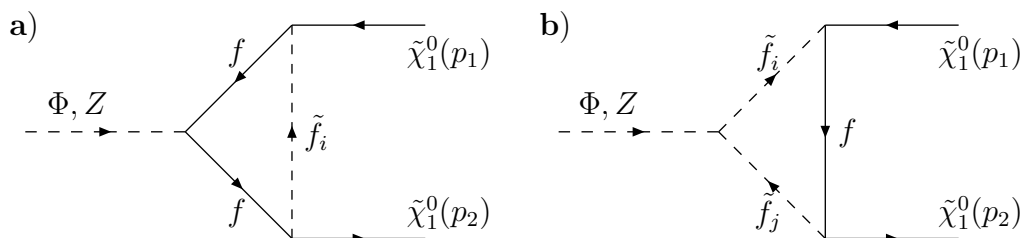


Figure 1: The Feynman diagrams contributing to the one-loop couplings of the lightest neutralinos to the Z and $\Phi = h, H, A$ Higgs bosons. Diagrams with crossed neutralino lines have to be added.

We have calculated the contributions of these diagrams for arbitrary momentum square of the Higgs and Z bosons, finite masses for the internal fermions and sfermions as well as for the external LSP neutralinos, and taking into account the full mixing in the sfermion sector. The amplitudes are ultra-violet finite as it should be. The contributions from diagrams a) and b) to the $\Phi\tilde{\chi}_1^0\tilde{\chi}_1^0$ couplings are separately finite for each fermion species.⁵ The $Z\tilde{\chi}_1^0\tilde{\chi}_1^0$ couplings are finite once contributions from both sfermion mass eigenstates of a given flavor and from both diagrams in Fig. 1 are added; diagrams a) and b) are separately finite after

⁴Loops containing charged gauge bosons and gauginos only can contribute to the $Z\tilde{\chi}_1^0\tilde{\chi}_1^0$ coupling if $\tilde{\chi}_1^0$ is wino-like. However, these contributions are separately gauge invariant only if the Z boson is on-shell. Since in this scenario $m_{\tilde{\chi}_1^\pm} \simeq m_{\tilde{\chi}_1^0}$, LEP searches imply that $\tilde{\chi}_1^0$ is too heavy to be produced in the decays of on-shell Z bosons. If the Z boson is off-shell, box-diagrams with two charged gauge bosons in the loop have to be added to obtain a gauge-invariant result.

⁵The contribution of diagram a) is finite only after summation over both sfermion mass eigenstates.

summation over a complete generation of (s)fermions. We have performed the calculation in the dimensional reduction scheme [14]; since the one-loop couplings are finite and do not require any renormalization, the same result is obtained using the dimensional regularization scheme [15], once the contributions from a complete SU(2) doublet have been added.⁶ The results are given below for a general gaugino ($|\mu| \gg M_1, M_2$, for arbitrary ordering of M_1 and M_2).

The one-loop induced Z boson vertex to a pair of lightest neutralinos is given by (p_1 is an incoming, p_2 an outgoing momentum):

$$\begin{aligned}\Gamma_\mu^1(Z\tilde{\chi}_1^0\tilde{\chi}_1^0) &= \frac{i}{4\pi^2} \frac{g}{c_W} \left\{ \gamma_\mu \gamma_5 \sum_f N_c^{(f)} \delta_a^{(f)} + (p_1 - p_2)_\mu \gamma_5 \sum_f N_c^{(f)} \delta_p^{(f)} \right\} \\ &\equiv ig_{Z\tilde{\chi}_1^0\tilde{\chi}_1^0}^1 \gamma_\mu \gamma_5 + ig_{Z\tilde{\chi}_1^0\tilde{\chi}_1^0}^p (p_1 - p_2)_\mu \gamma_5,\end{aligned}\quad (12)$$

with the color factors $N_c^{(f)}$, and

$$\begin{aligned}\delta_a^{(f)} &= (a_f + v_f c_{2\theta_{\tilde{f}}}) v_1 \left[-m_{\tilde{f}}^2 C_0(\tilde{f}_1) - m_{\tilde{\chi}_1^0}^2 C_0(\tilde{f}_2) + 4m_{\tilde{\chi}_1^0}^2 C_1^+(\tilde{f}_2) \right. \\ &\quad \left. - 2(m_{\tilde{\chi}_1^0}^2 + p_1 \cdot p_2) C_2^+(\tilde{f}_2) - 2(m_{\tilde{\chi}_1^0}^2 - p_1 \cdot p_2) C_2^-(\tilde{f}_2) - 2C_2^0(\tilde{f}_2) \right] \\ &+ (a_f - v_f c_{2\theta_{\tilde{f}}}) v_1 \left[-m_{\tilde{f}}^2 C_0(\tilde{f}_2) - m_{\tilde{\chi}_1^0}^2 C_0(\tilde{f}_1) + 4m_{\tilde{\chi}_1^0}^2 C_1^+(\tilde{f}_1) \right. \\ &\quad \left. - 2(m_{\tilde{\chi}_1^0}^2 + p_1 \cdot p_2) C_2^+(\tilde{f}_1) - 2(m_{\tilde{\chi}_1^0}^2 - p_1 \cdot p_2) C_2^-(\tilde{f}_1) - 2C_2^0(\tilde{f}_1) \right] \\ &+ 2m_{\tilde{f}} m_{\tilde{\chi}_1^0} a_f s_{2\theta_{\tilde{f}}} (v_1 + v_3) \left[C_0(\tilde{f}_1) - C_0(\tilde{f}_2) - 2C_1^+(\tilde{f}_1) + 2C_1^+(\tilde{f}_2) \right] \\ &- (a_f + v_f) v_2 m_{\tilde{f}}^2 \left[C_0(\tilde{f}_1) c_{\theta_{\tilde{f}}}^2 + C_0(\tilde{f}_2) s_{\theta_{\tilde{f}}}^2 \right] \\ &+ (a_f - v_f) v_2 \left[c_{\theta_{\tilde{f}}}^2 \left(-m_{\tilde{\chi}_1^0}^2 C_0(\tilde{f}_1) + 4m_{\tilde{\chi}_1^0}^2 C_1^+(\tilde{f}_1) - 2C_2^0(\tilde{f}_1) \right. \right. \\ &\quad \left. \left. - 2(m_{\tilde{\chi}_1^0}^2 + p_1 \cdot p_2) C_2^+(\tilde{f}_1) - 2(m_{\tilde{\chi}_1^0}^2 - p_1 \cdot p_2) C_2^-(\tilde{f}_1) \right) \right. \\ &\quad \left. + s_{\theta_{\tilde{f}}}^2 \left(-m_{\tilde{\chi}_1^0}^2 C_0(\tilde{f}_2) + 4m_{\tilde{\chi}_1^0}^2 C_1^+(\tilde{f}_2) - 2C_2^0(\tilde{f}_2) \right. \right. \\ &\quad \left. \left. - 2(m_{\tilde{\chi}_1^0}^2 + p_1 \cdot p_2) C_2^+(\tilde{f}_2) - 2(m_{\tilde{\chi}_1^0}^2 - p_1 \cdot p_2) C_2^-(\tilde{f}_2) \right) \right] \\ &- c_{2\theta_{\tilde{f}}} v_1 \left[f_{Z\tilde{f}_1\tilde{f}_1} C_2^0(\tilde{f}_1, \tilde{f}_1) - f_{Z\tilde{f}_2\tilde{f}_2} C_2^0(\tilde{f}_2, \tilde{f}_2) \right] \\ &- v_2 \left[c_{\theta_{\tilde{f}}}^2 f_{Z\tilde{f}_1\tilde{f}_1} C_2^0(\tilde{f}_1, \tilde{f}_1) + s_{\theta_{\tilde{f}}}^2 f_{Z\tilde{f}_2\tilde{f}_2} C_2^0(\tilde{f}_2, \tilde{f}_2) \right] \\ &+ s_{2\theta_{\tilde{f}}} (2v_1 + v_2) f_{Z\tilde{f}_1\tilde{f}_2} C_2^0(\tilde{f}_1, \tilde{f}_2); \end{aligned}\quad (13)$$

$$\begin{aligned}\delta_p^{(f)} &= (a_f + v_f c_{2\theta_{\tilde{f}}}) 2m_{\tilde{\chi}_1^0} v_1 \left[C_1^+(\tilde{f}_2) - 2C_2^-(\tilde{f}_2) \right] \\ &+ (a_f - v_f c_{2\theta_{\tilde{f}}}) 2m_{\tilde{\chi}_1^0} v_1 \left[C_1^+(\tilde{f}_1) - 2C_2^-(\tilde{f}_1) \right] \\ &+ 2a_f s_{2\theta_{\tilde{f}}} (v_1 + v_3) m_{\tilde{f}} \left[-C_1^+(\tilde{f}_1) + C_1^+(\tilde{f}_2) \right]\end{aligned}$$

⁶In the $\overline{\text{MS}}$ scheme the contribution from a given fermion species contains mass-independent terms proportional to some combinations of Zff couplings. These constant terms add to zero when summed over a complete generation of fermions and sfermions.

$$\begin{aligned}
& + 2(a_f - v_f)v_2 m_{\tilde{\chi}_1^0} \left[c_{\theta_{\tilde{f}}}^2 (C_1^+(\tilde{f}_1) - 2C_2^-(\tilde{f}_1)) + s_{\theta_{\tilde{f}}}^2 (C_1^+(\tilde{f}_2) - 2C_2^-(\tilde{f}_2)) \right] \\
& + 2c_{2\theta_{\tilde{f}}} v_1 m_{\tilde{\chi}_1^0} \left[f_{Z\tilde{f}_1\tilde{f}_1} C_2^-(\tilde{f}_1, \tilde{f}_1) - f_{Z\tilde{f}_2\tilde{f}_2} C_2^-(\tilde{f}_2, \tilde{f}_2) \right] \\
& + 2v_2 m_{\tilde{\chi}_1^0} \left[c_{\theta_{\tilde{f}}}^2 f_{Z\tilde{f}_1\tilde{f}_1} C_2^-(\tilde{f}_1, \tilde{f}_1) + s_{\theta_{\tilde{f}}}^2 f_{Z\tilde{f}_2\tilde{f}_2} C_2^-(\tilde{f}_2, \tilde{f}_2) \right] \\
& + 2f_{Z\tilde{f}_1\tilde{f}_2} \left[(v_1 + v_3)m_f C_1^-(\tilde{f}_1, \tilde{f}_2) - s_{2\theta_{\tilde{f}}}(2v_1 + v_2)m_{\tilde{\chi}_1^0} C_2^-(\tilde{f}_1, \tilde{f}_2) \right]. \tag{14}
\end{aligned}$$

Here we have used the notation

$$\begin{aligned}
v_f &= -\frac{1}{2}I_3^f + s_W^2 Q_f, \quad a_f = \frac{1}{2}I_3^f, \\
v_0 &= (gQ_f N_{11} \tan \theta_W)^2, \quad v_1 = \frac{1}{2}v_0, \\
v_2 &= \frac{I_3^f}{2Q_f} v_0 \left[-2 + \frac{I_3^f}{Q_f} + 2 \left(1 - \frac{I_3^f}{Q_f} \right) \frac{N_{12}}{N_{11} \tan \theta_W} + \frac{I_3^f}{Q_f} \left(\frac{N_{12}}{N_{11} \tan \theta_W} \right)^2 \right], \\
v_3 &= \frac{I_3^f}{2Q_f} v_0 \left(\frac{N_{12}}{N_{11} \tan \theta_W} - 1 \right). \tag{15}
\end{aligned}$$

The Z boson couplings to sfermions are given by:

$$f_{Z\tilde{f}_1\tilde{f}_1} = -2I_3^f c_{\theta_{\tilde{f}}}^2 + 2Q_f s_W^2, \quad f_{Z\tilde{f}_2\tilde{f}_2} = -2I_3^f s_{\theta_{\tilde{f}}}^2 + 2Q_f s_W^2, \quad f_{Z\tilde{f}_1\tilde{f}_2} = I_3^f s_{2\theta_{\tilde{f}}}. \tag{16}$$

The angle $\theta_{\tilde{f}}$ is the mixing angle arising from the diagonalization of the sfermion mass matrices [compare eq. (24) below] and $s_{\theta_{\tilde{f}}}^2 = 1 - c_{\theta_{\tilde{f}}}^2 \equiv \sin^2 \theta_{\tilde{f}}$. Q_f and I_3^f denote the electric charge and weak isospin of the fermion f , respectively. The Passarino–Veltman three-point functions [16], defined as

$$\begin{aligned}
C_{0,1,2}^{0,+,-}(\tilde{f}) &\equiv C_{0,1,2}^{0,+,-}(q^2, m_{\tilde{\chi}_1^0}^2, m_f^2, m_f^2, m_{\tilde{f}}^2); \\
C_{0,1,2}^{0,+,-}(\tilde{f}_1, \tilde{f}_2) &\equiv C_{0,1,2}^{0,+,-}(q^2, m_{\tilde{\chi}_1^0}^2, m_{\tilde{f}_1}^2, m_{\tilde{f}_2}^2, m_f^2), \tag{17}
\end{aligned}$$

with q the momentum of the Higgs or Z boson, can be found in Ref. [13].⁷

In the same notation, the one-loop Higgs boson couplings to the LSP neutralinos in the bino limit are given by:

$$\begin{aligned}
\Gamma^1(\phi \tilde{\chi}_1^0 \tilde{\chi}_1^0) &= \frac{ig}{4\pi^2} \left[\sum_f N_c \delta_\phi^{(f)} \right] \equiv ig_{\phi \tilde{\chi}_1^0 \tilde{\chi}_1^0}^1 \\
\Gamma^1(A \tilde{\chi}_1^0 \tilde{\chi}_1^0) &= \frac{g}{4\pi^2} \gamma_5 \left[\sum_f N_c \delta_A^{(f)} \right] \equiv g_{A \tilde{\chi}_1^0 \tilde{\chi}_1^0}^1 \gamma_5 \tag{18}
\end{aligned}$$

⁷Some care has to be taken if $q^2 \rightarrow 0$ or $q^2 = 4m_{\tilde{\chi}_1^0}^2$, since standard expressions for the loop functions contain spurious divergences in these kinematical situations, which are characteristic for LSP–nucleus scattering and LSP annihilation, respectively. This problem is discussed in the Appendix of Ref. [13].

where

$$\begin{aligned}
\delta_\phi^{(f)} = & \frac{m_f g_{\phi f f}}{2m_W} \left\{ s_{2\theta_{\tilde{f}}}(v_1 + v_3) \left[- \left(m_{\tilde{f}_1}^2 + m_f^2 + m_{\tilde{\chi}_1^0}^2 \right) C_0(\tilde{f}_1) + 4m_{\tilde{\chi}_1^0}^2 C_1^+(\tilde{f}_1) \right. \right. \\
& + \left. \left(m_{\tilde{f}_2}^2 + m_f^2 + m_{\tilde{\chi}_1^0}^2 \right) C_0(\tilde{f}_2) - 4m_{\tilde{\chi}_1^0}^2 C_1^+(\tilde{f}_2) \right] \\
& + 2(v_1 + v_2 c_{\theta_{\tilde{f}}}^2) m_f m_{\tilde{\chi}_1^0} \left[C_0(\tilde{f}_1) - 2C_1^+(\tilde{f}_1) \right] \\
& + 2(v_1 + v_2 s_{\theta_{\tilde{f}}}^2) m_f m_{\tilde{\chi}_1^0} \left[C_0(\tilde{f}_2) - 2C_1^+(\tilde{f}_2) \right] \Big\} \\
& - C_{\phi \tilde{f}_1 \tilde{f}_1} \left\{ -s_{2\theta_{\tilde{f}}}(v_1 + v_3) m_f C_0(\tilde{f}_1, \tilde{f}_1) + 2(v_1 + v_2 c_{\theta_{\tilde{f}}}^2) m_{\tilde{\chi}_1^0} C_1^+(\tilde{f}_1, \tilde{f}_1) \right\} \\
& - C_{\phi \tilde{f}_2 \tilde{f}_2} \left\{ s_{2\theta_{\tilde{f}}}(v_1 + v_3) m_f C_0(\tilde{f}_2, \tilde{f}_2) + 2(v_1 + v_2 s_{\theta_{\tilde{f}}}^2) m_{\tilde{\chi}_1^0} C_1^+(\tilde{f}_2, \tilde{f}_2) \right\} \\
& - C_{\phi \tilde{f}_1 \tilde{f}_2} \left\{ -2c_{2\theta_{\tilde{f}}}(v_1 + v_3) m_f C_0(\tilde{f}_1, \tilde{f}_2) - 2s_{2\theta_{\tilde{f}}} v_2 m_{\tilde{\chi}_1^0} C_1^+(\tilde{f}_1, \tilde{f}_2) \right\}; \tag{19}
\end{aligned}$$

$$\begin{aligned}
\delta_A^{(f)} = & \frac{m_f g_{A f f}}{2m_W} \left\{ (v_1 + v_3) s_{2\theta_{\tilde{f}}} \left[\left(m_{\tilde{f}_1}^2 - m_f^2 - m_{\tilde{\chi}_1^0}^2 \right) C_0(\tilde{f}_1) - \left(m_{\tilde{f}_2}^2 - m_f^2 - m_{\tilde{\chi}_1^0}^2 \right) C_0(\tilde{f}_2) \right] \right. \\
& + 2(v_1 + v_2 c_{\theta_{\tilde{f}}}^2) m_{\tilde{\chi}_1^0} m_f C_0(\tilde{f}_1) + 2(v_1 + v_2 s_{\theta_{\tilde{f}}}^2) m_{\tilde{\chi}_1^0} m_f C_0(\tilde{f}_2) \Big\} \\
& + C_{A \tilde{f}_1 \tilde{f}_2} \left\{ -2m_f (v_1 + v_3) C_0(\tilde{f}_1, \tilde{f}_2) + 2m_{\tilde{\chi}_1^0} (2v_1 + v_2) s_{2\theta_{\tilde{f}}} C_1^-(\tilde{f}_1, \tilde{f}_2) \right\}. \tag{20}
\end{aligned}$$

The Higgs–fermion–fermion coupling constants are given by

$$\begin{aligned}
g_{h u u} &= \frac{\cos \alpha}{\sin \beta} \quad , \quad g_{h d d} = \frac{-\sin \alpha}{\cos \beta} \quad , \\
g_{H u u} &= \frac{\sin \alpha}{\sin \beta} \quad , \quad g_{H d d} = \frac{\cos \alpha}{\cos \beta} \quad , \\
g_{A u u} &= \cot \beta \quad , \quad g_{A d d} = \tan \beta \quad , \tag{21}
\end{aligned}$$

while the Higgs–sfermion–sfermion coupling constants read:

$$\begin{aligned}
C_{h \tilde{u}_1 \tilde{u}_1} &= \frac{m_Z}{c_W} s_{\beta+\alpha} \left[I_3^u c_{\theta_{\tilde{u}}}^2 - Q_u s_W^2 c_{2\theta_{\tilde{u}}} \right] - \frac{m_u^2 g_{h u u}}{m_W} - \frac{m_u s_{2\theta_{\tilde{u}}}}{2m_W} [A_u g_{h u u} + \mu g_{H u u}]; \\
C_{h \tilde{u}_2 \tilde{u}_2} &= \frac{m_Z}{c_W} s_{\beta+\alpha} \left[I_3^u s_{\theta_{\tilde{u}}}^2 + Q_u s_W^2 c_{2\theta_{\tilde{u}}} \right] - \frac{m_u^2 g_{h u u}}{m_W} + \frac{m_u s_{2\theta_{\tilde{u}}}}{2m_W} [A_u g_{h u u} + \mu g_{H u u}]; \\
C_{h \tilde{u}_1 \tilde{u}_2} &= \frac{m_Z}{c_W} s_{\beta+\alpha} \left[Q_u s_W^2 - I_3^u / 2 \right] s_{2\theta_{\tilde{u}}} - \frac{m_u}{2m_W} [A_u g_{h u u} + \mu g_{H u u}] c_{2\theta_{\tilde{u}}}; \\
C_{h \tilde{d}_1 \tilde{d}_1} &= \frac{m_Z}{c_W} s_{\beta+\alpha} \left[I_3^d c_{\theta_{\tilde{d}}}^2 - Q_d s_W^2 c_{2\theta_{\tilde{d}}} \right] - \frac{m_d^2 g_{h d d}}{m_W} - \frac{m_d s_{2\theta_{\tilde{d}}}}{2m_W} [A_d g_{h d d} - \mu g_{H d d}]; \\
C_{h \tilde{d}_2 \tilde{d}_2} &= \frac{m_Z}{c_W} s_{\beta+\alpha} \left[I_3^d s_{\theta_{\tilde{d}}}^2 + Q_d s_W^2 c_{2\theta_{\tilde{d}}} \right] - \frac{m_d^2 g_{h d d}}{m_W} + \frac{m_d s_{2\theta_{\tilde{d}}}}{2m_W} [A_d g_{h d d} - \mu g_{H d d}]; \\
C_{h \tilde{d}_1 \tilde{d}_2} &= \frac{m_Z}{c_W} s_{\beta+\alpha} \left[Q_d s_W^2 - I_3^d / 2 \right] s_{2\theta_{\tilde{d}}} - \frac{m_d}{2m_W} [A_d g_{h d d} - \mu g_{H d d}] c_{2\theta_{\tilde{d}}}; \\
C_{H \tilde{u}_1 \tilde{u}_1} &= -\frac{m_Z}{c_W} c_{\beta+\alpha} \left[I_3^u c_{\theta_{\tilde{u}}}^2 - Q_u s_W^2 c_{2\theta_{\tilde{u}}} \right] - \frac{m_u^2 g_{H u u}}{m_W} - \frac{m_u s_{2\theta_{\tilde{u}}}}{2m_W} [A_u g_{H u u} - \mu g_{h u u}];
\end{aligned}$$

$$\begin{aligned}
C_{H\tilde{u}_2\tilde{u}_2} &= -\frac{m_Z}{c_W}c_{\beta+\alpha}\left[I_3^u s_{\theta_{\tilde{u}}}^2 + Q_u s_W^2 c_{2\theta_{\tilde{u}}}\right] - \frac{m_u^2 g_{Huu}}{m_W} + \frac{m_u s_{2\theta_{\tilde{u}}}}{2m_W} [A_u g_{Huu} - \mu g_{huu}]; \\
C_{H\tilde{u}_1\tilde{u}_2} &= -\frac{m_Z}{c_W}c_{\beta+\alpha}\left[Q_u s_W^2 - I_3^u/2\right] s_{2\theta_{\tilde{u}}} - \frac{m_u}{2m_W} [A_u g_{Huu} - \mu g_{huu}] c_{2\theta_{\tilde{u}}}; \\
C_{H\tilde{d}_1\tilde{d}_1} &= -\frac{m_Z}{c_W}c_{\beta+\alpha}\left[I_3^d c_{\theta_{\tilde{d}}}^2 - Q_d s_W^2 c_{2\theta_{\tilde{d}}}\right] - \frac{m_d^2 g_{Hdd}}{m_W} - \frac{m_d s_{2\theta_{\tilde{d}}}}{2m_W} [A_d g_{Hdd} + \mu g_{hdd}]; \\
C_{H\tilde{d}_2\tilde{d}_2} &= -\frac{m_Z}{c_W}c_{\beta+\alpha}\left[I_3^d s_{\theta_{\tilde{d}}}^2 + Q_d s_W^2 c_{2\theta_{\tilde{d}}}\right] - \frac{m_d^2 g_{Hdd}}{m_W} + \frac{m_d s_{2\theta_{\tilde{d}}}}{2m_W} [A_d g_{Hdd} + \mu g_{hdd}]; \\
C_{H\tilde{d}_1\tilde{d}_2} &= -\frac{m_Z}{c_W}c_{\beta+\alpha}\left[Q_d s_W^2 - I_3^d/2\right] s_{2\theta_{\tilde{d}}} - \frac{m_d}{2m_W} [A_d g_{Hdd} + \mu g_{hdd}] c_{2\theta_{\tilde{d}}}; \\
C_{A\tilde{u}_1\tilde{u}_2} &= \frac{m_u}{2m_W}(A_u \cot \beta + \mu); \\
C_{A\tilde{d}_1\tilde{d}_2} &= \frac{m_d}{2m_W}(A_d \tan \beta + \mu).
\end{aligned} \tag{22}$$

We use the following convention for the sfermion mass matrices:

$$\mathcal{M}_f^2 = \begin{pmatrix} m_f^2 + m_{LL}^2 & m_f \tilde{A}_f \\ m_f \tilde{A}_f & m_f^2 + m_{RR}^2 \end{pmatrix}, \quad \text{with} \quad \begin{aligned} m_{LL}^2 &= m_{\tilde{f}_L}^2 + (I_3^f - Q_f s_W^2) m_Z^2 c_{2\beta} \\ m_{RR}^2 &= m_{\tilde{f}_R}^2 + Q_f s_W^2 m_Z^2 c_{2\beta} \\ \tilde{A}_f &= A_f - \mu(\tan \beta)^{-2I_3^f} \end{aligned} \tag{23}$$

They are diagonalized by 2×2 rotation matrices described by the angles $\theta_{\tilde{f}}$, which turn the current eigenstates, \tilde{f}_L and \tilde{f}_R , into the mass eigenstates \tilde{f}_1 and \tilde{f}_2 ; the mixing angle and sfermion masses are then given by

$$s_{2\theta_{\tilde{f}}} = \frac{2m_f \tilde{A}_f}{m_{\tilde{f}_1}^2 - m_{\tilde{f}_2}^2}, \quad c_{2\theta_{\tilde{f}}} = \frac{m_{LL}^2 - m_{RR}^2}{m_{\tilde{f}_1}^2 - m_{\tilde{f}_2}^2}, \tag{24}$$

$$m_{\tilde{f}_{1,2}}^2 = m_f^2 + \frac{1}{2} \left[m_{LL}^2 + m_{RR}^2 \mp \sqrt{(m_{LL}^2 - m_{RR}^2)^2 + 4m_f^2 \tilde{A}_f^2} \right]. \tag{25}$$

3 Higgs and Z Boson Decays

3.1 Invisible decays of the Z boson

The tree level and the one-loop induced axial vector couplings of the Z boson to $\tilde{\chi}_1^0$ pairs are shown in Fig. 2a for the input values $\tan \beta = 15$ and $\mu = 1$ TeV. We work in an unconstrained model with non-universal boundary conditions for the gaugino mass parameters at the high energy scale,⁸ and set the bino and wino mass parameters to $M_1 = 30$ GeV and $M_2 = 120$ GeV, respectively. For definiteness we assume a common soft SUSY breaking scalar mass for the three generations of sleptons, $m_{\tilde{e}_L} = m_{\tilde{e}_R} \equiv m_{\tilde{l}}$, and a common mass term for the squarks $m_{\tilde{q}_L} = m_{\tilde{u}_R} = m_{\tilde{d}_R} \equiv m_{\tilde{q}}$, with $m_{\tilde{q}} = 2m_{\tilde{l}}$. For the trilinear coupling, which will play

⁸In models with universal gaugino masses at the GUT scale, the bound on the lightest chargino mass from negative searches at LEP2, $m_{\tilde{\chi}_1^\pm} \gtrsim 104$ GeV [17, 18], will constrain a bino-like neutralino to have a mass larger than $m_Z/2$; the decay $Z \rightarrow \tilde{\chi}_1^0 \tilde{\chi}_1^0$ would then be kinematically closed.

a role mainly in the stop sector, we choose the value $A_t = 2.9m_{\tilde{q}}$. The trilinear couplings in the \tilde{d} -squark and slepton sectors, which are not important here, have been set to zero.

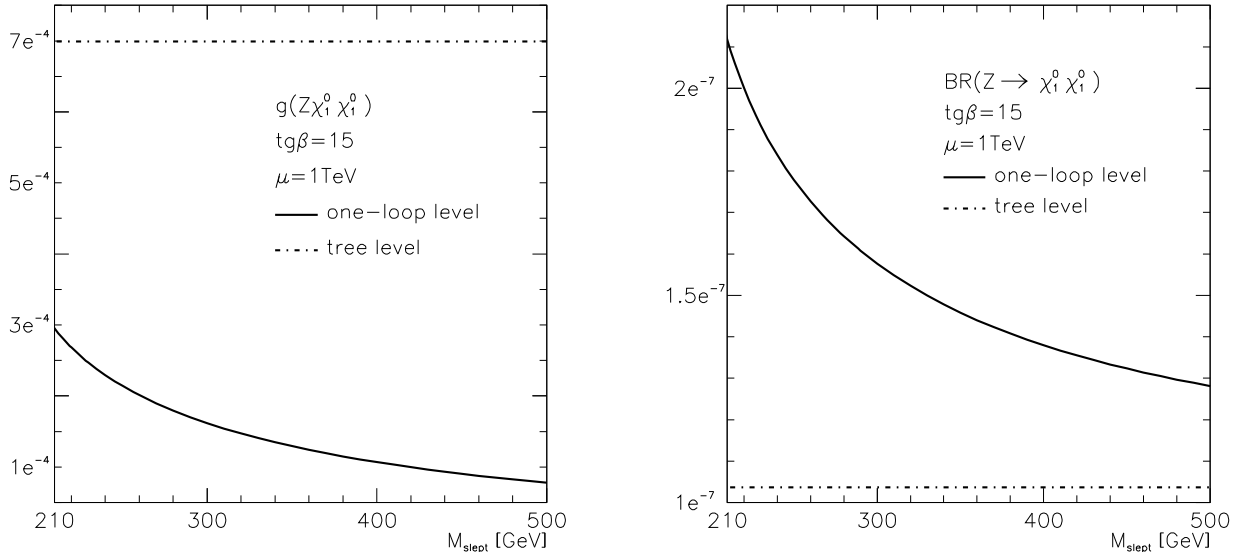


Figure 2: The Z boson axial vector coupling (left) and branching ratio (right) to pairs of the lightest neutralino as functions of the common slepton mass. The dashed lines show the tree-level results; the solid line in the left frame shows the real part of the one-loop contribution eq. (12) to the axial vector coupling, while the solid line in the right frame shows the total loop-corrected branching ratio eq. (26). These results are given for $\tan\beta = 15$, $\mu = 1$ TeV, $m_{\tilde{q}} = 2m_{\tilde{l}}$, $A_t = 2.9m_{\tilde{q}}$ and gaugino masses $M_1 = 30$ GeV, $M_2 = 120$ GeV.

The tree-level coupling $g_{Z\tilde{\chi}_1^0\tilde{\chi}_1^0}^0$ is very small if $\tilde{\chi}_1^0$ is bino-like, being of $\mathcal{O}(m_Z^2/\mu^2)$. As can be seen from Fig. 2a, it is less than 10^{-3} for the chosen parameters [and of course does not depend on slepton and squark masses]. The real part of the one-loop induced coupling, $g_{Z\tilde{\chi}_1^0\tilde{\chi}_1^0}^1$, for on-shell Z bosons [i.e. with $q^2 = m_Z^2$] receives contributions from both massless and massive SM fermions and their superpartners. In the former case the real part has an “accidental” zero for sfermion masses slightly above the Z mass; this happens e.g. for the (s)neutrino contribution at $m_{\tilde{\nu}} \simeq 94$ GeV.⁹ The real part of this contribution is positive (negative) for smaller (larger) sneutrino masses; its absolute value reaches a maximum at $m_{\tilde{\nu}} \simeq 155$ GeV. No such zero occurs for the imaginary parts. Moreover, the (s)top loop contribution is much larger than that from the other (s)quarks, even if the stop masses are not reduced significantly compared to the other squark masses. When combined with the “accidental” suppression of the (s)lepton contribution for slepton masses close to their present lower experimental bound, this implies that the dominant contribution to the real part of this coupling usually comes from (s)top loops. Of course, these loops cannot contribute to

⁹This statement holds, strictly speaking, only in the $\overline{\text{MS}}$ scheme, where the contribution from each (s)fermion species decouples separately when $m_{\tilde{f}} \rightarrow \infty$. In the $\overline{\text{DR}}$ scheme decoupling only occurs after summation over a complete generation.

the imaginary part, which receives its dominant contribution from (s)lepton loops. For large masses, sparticles decouple and the loop correction to the coupling vanishes asymptotically.

The partial decay width for the decay of a Z boson into a pair of LSP neutralinos is given by:

$$\Gamma(Z \rightarrow \tilde{\chi}_1^0 \tilde{\chi}_1^0) = \frac{\beta_Z^3 m_Z}{24\pi} \left| g_{Z\tilde{\chi}_1^0 \tilde{\chi}_1^0}^0 + g_{Z\tilde{\chi}_1^0 \tilde{\chi}_1^0}^1 \right|^2, \quad (26)$$

where $\beta_Z = (1 - 4m_{\tilde{\chi}_1^0}^2/m_Z^2)^{1/2}$ is the velocity of the neutralinos in the rest frame of the Z boson. In the usual perturbative expansion the one-loop correction to a decay width originates from the interference of tree-level diagrams with the real parts of the corresponding one-loop diagrams. However, in our case the tree-level decay width will vanish in the limit $|\mu| \rightarrow \infty$. In this limit the one-loop diagrams represent the leading order contributions. We therefore also include the squared one-loop contribution in eq. (26). However, for $|\mu| \lesssim 1$ TeV the numerically most important correction to the tree-level result usually still comes from the interference between the tree level and the real part of the one-loop couplings. Note finally that the derivative coupling $g_{Z\tilde{\chi}_1^0 \tilde{\chi}_1^0}^p$ of eq. (12) does not contribute to the decay width of real Z bosons, since the product of the Z polarization vector with the sum of the outgoing LSP momenta vanishes.

The Z decay branching ratio, $\text{BR}(Z \rightarrow \tilde{\chi}_1^0 \tilde{\chi}_1^0) = \Gamma(Z \rightarrow \tilde{\chi}_1^0 \tilde{\chi}_1^0)/\Gamma_Z^{\text{tot}}$ with $\Gamma_Z^{\text{tot}} = 2.5$ GeV, is shown in Fig. 2b. In the Born approximation, the branching ratio is very small, $\sim 1 \cdot 10^{-7}$. It can be enhanced by the loop contribution by a factor of $\gtrsim 2$ in the low slepton mass range. However, the branching fraction is still well below the experimental limit on the invisible Z boson decay width [17],

$$\Delta\Gamma_Z^{\text{inv}}|_{\text{exp}} \simeq \pm 1.5 \text{ MeV}, \quad (27)$$

which would require a branching ratio in the permille range for detection. One can find scenarios with somewhat larger loop corrections than shown in Fig. 2, if parameters are chosen such that all slepton masses are near 150 GeV. However, even in this case we are still more than three orders of magnitude below the experimental limit (27). Of course the Z partial decay width into $\tilde{\chi}_1^0$ pairs can be enhanced to a detectable level for lower values of the parameter μ . However, in this case the one-loop corrections [which remain more or less the same] would be relatively less important than for large $|\mu|$.

3.2 Invisible decays of the Higgs bosons

The real part of the coupling of an on-shell lightest h boson to a $\tilde{\chi}_1^0$ pair is displayed, at the Born and one-loop level, in the left-hand frames of Figs. 3. It is again shown as a function of the sfermion masses, for $\tan\beta = 15$, $\mu = 1$ TeV and pseudoscalar mass input values $M_A = 200$ GeV (upper frames) and 1 TeV (lower frames). We see that the tree-level coupling $g_{h\tilde{\chi}_1^0 \tilde{\chi}_1^0}^0$ is typically a factor of three larger than the corresponding coupling $g_{Z\tilde{\chi}_1^0 \tilde{\chi}_1^0}^0$ of the Z boson. This can be understood from eqs. (1), (2) and (7). In the “decoupling” limit $M_A^2 \gg m_Z^2$ the neutral Higgs mixing angle α satisfies $s_\alpha = -c_\beta$, $c_\alpha = s_\beta$. In this limit

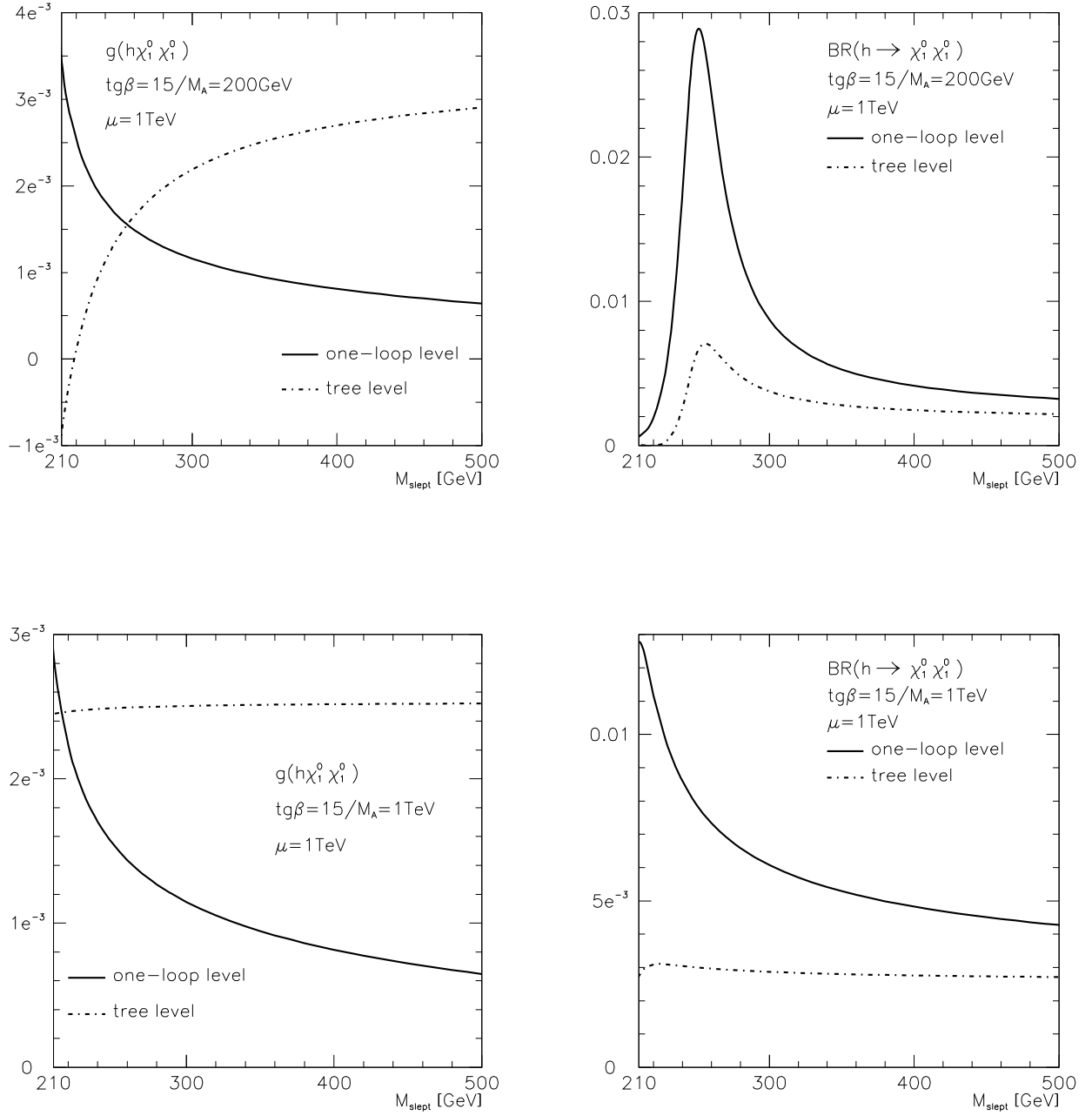


Figure 3: The lightest h boson couplings (left) and branching ratios (right) to pairs of the lightest neutralinos as functions of the common slepton mass. Most parameters are as in Fig. 2, and we took $M_A = 200$ GeV (top) and 1 TeV (bottom).

the ratio of tree-level $Z\tilde{\chi}_1^0\tilde{\chi}_1^0$ and $h\tilde{\chi}_1^0\tilde{\chi}_1^0$ couplings becomes $-m_Z \cot 2\beta/(2\mu)$; for the given choice of parameters this amounts to about 0.3, in good agreement with Figs. 2 and 3. On the other hand, for small sfermion masses the one-loop corrections to the $h\tilde{\chi}_1^0\tilde{\chi}_1^0$ coupling exceed $g_{Z\tilde{\chi}_1^0\tilde{\chi}_1^0}^1$ by more than an order of magnitude. The corrections to the Z coupling to bino-like neutralinos only involve electroweak gauge couplings. In contrast, top quarks couple with $\mathcal{O}(1)$ Yukawa coupling to the Higgs bosons, and for the given choice of large $|A_t|$ the (dimensionful) $h\tilde{t}_1\tilde{t}_1$ coupling significantly exceeds the \tilde{t}_1 mass. Moreover, due to $\tilde{t}_L - \tilde{t}_R$ mixing the lighter \tilde{t} mass eigenstate is often not only lighter than the other squarks, but also lighter than the sleptons. As a result, the loop corrections are numerically even *more* important in case of the Higgs coupling, even though the tree-level contribution to this coupling is nominally only suppressed by one power of $|\mu|$. If $|A_t|$ is large, as in the present example, the loop corrections to the $h\tilde{\chi}_1^0\tilde{\chi}_1^0$ coupling can even exceed the tree-level contribution.

The variation of the one-loop contribution to the coupling is again mostly due to the natural decrease with increasing masses of the sfermions running in the loop, which decouple when they are much heavier than the h boson. For $m_{\tilde{q}} \simeq 420$ GeV [i.e. $m_{\tilde{l}} \simeq 210$ GeV], $m_{\tilde{t}_1}$ is near its experimental lower bound of ~ 100 GeV, due to strong $\tilde{t}_L - \tilde{t}_R$ mixing. This implies that $m_{\tilde{t}_1}$ will grow faster than linearly with increasing $m_{\tilde{q}}$, which explains the very rapid decrease of the loop corrections. However, there is also a variation of the tree-level coupling for $M_A = 200$ GeV which, at first sight, is astonishing. It is caused by the variation of the mixing angle α in the CP-even Higgs sector, and to a lesser extent by the variation of M_h , due to the strong dependence of crucial loop corrections in the CP-even Higgs sector on the stop masses.¹⁰ In fact, for the set of input parameters with $M_A = 200$ GeV at small slepton masses, we are in the regime where $\sin \alpha$, which appears in the $h\tilde{\chi}_1^0\tilde{\chi}_1^0$ coupling [and which enters the $h\tilde{b}\tilde{b}$ coupling as will be discussed later], varies very quickly. This “pathological” region, where the phenomenology of the MSSM Higgs bosons is drastically affected, has been discussed in several places in the literature [19].

The partial widths for the decays of CP-even Higgs bosons, $\phi = h, H$, into pairs of identical neutralinos are given by [20]:

$$\Gamma(\phi \rightarrow \tilde{\chi}_1^0\tilde{\chi}_1^0) = \frac{\beta_\phi^3 M_\phi}{16\pi} |g_{\phi\tilde{\chi}_1^0\tilde{\chi}_1^0}^0 + g_{\phi\tilde{\chi}_1^0\tilde{\chi}_1^0}^1|^2. \quad (28)$$

The branching ratios for the decays of the lightest h boson are shown in the right-hand frames of Figs. 3 for the same choice of parameters previously discussed. They have been calculated by implementing the one-loop Higgs couplings to neutralinos in the Fortran code **HDECAY** [21] which calculates all possible decays of the MSSM Higgs bosons and where all important corrections in the Higgs sector, in both the spectrum and the various decay widths, are included. We see that the situation is completely different from the case of the decay $Z \rightarrow \tilde{\chi}_1^0\tilde{\chi}_1^0$: the branching ratio $\text{BR}(h \rightarrow \tilde{\chi}_1^0\tilde{\chi}_1^0)$ can already exceed the one permille level with tree-level couplings. This enhancement is not only due the larger $g_{h\tilde{\chi}_1^0\tilde{\chi}_1^0}$ couplings

¹⁰We remind the reader that LEP Higgs searches would completely exclude the MSSM in the absence of these corrections.

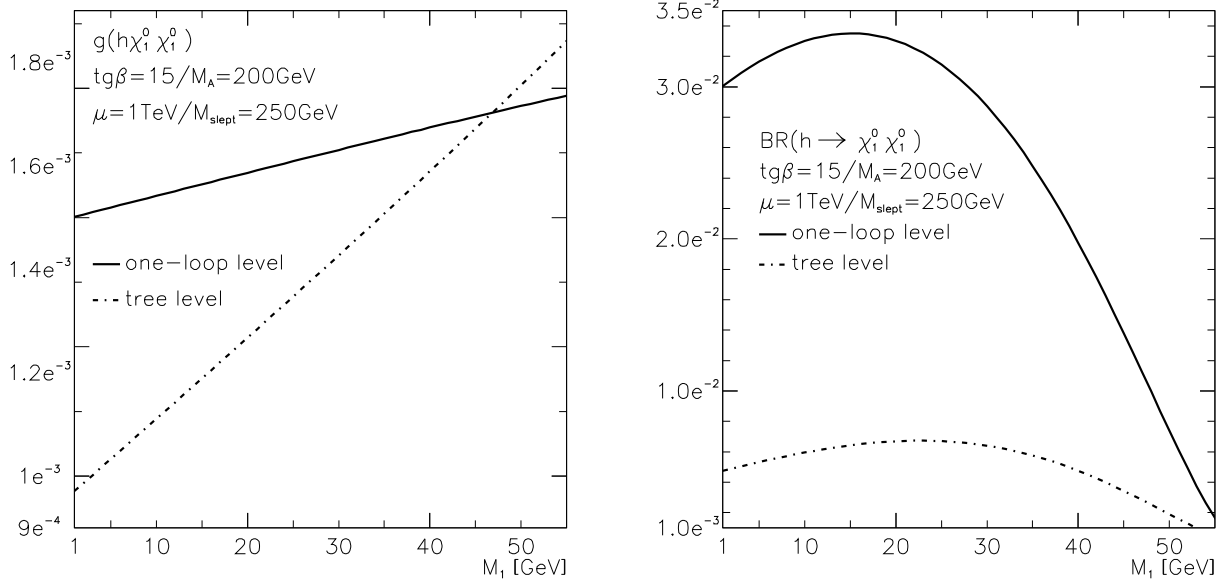


Figure 4: The lightest h boson couplings (left) and branching ratios (right) to pairs of the lightest neutralinos as functions of M_1 . The parameters are as in Fig. 2 with $m_{\tilde{l}} = 250$ GeV and $M_A = 200$ GeV.

compared to $g_{Z\tilde{\chi}_1^0\tilde{\chi}_1^0}$, but also due to the much smaller h total decay width¹¹, $\Gamma_h^{\text{tot}} \sim$ a few MeV, compared to $\Gamma_Z^{\text{tot}} \simeq 2.5$ GeV. After including the one-loop corrections, the branching fraction $BR(h \rightarrow \tilde{\chi}_1^0\tilde{\chi}_1^0)$ can be enhanced to reach the level of a few percent.

The branching ratio is especially enhanced if the usually dominant decay into $b\bar{b}$ pairs is suppressed, i.e. if $|\sin\alpha|$ is very small; recall that the $hb\bar{b}$ coupling is $\propto \sin\alpha/\cos\beta$. In our examples this happens for $M_A = 200$ GeV and $m_{\tilde{l}} \simeq 250$ GeV. In this case $g_{h\tilde{\chi}_1^0\tilde{\chi}_1^0}^0$ is only about half as large as in the decoupling limit $M_A \rightarrow \infty$, but the loop contribution to this coupling is still sizable for this value of the sfermion masses, and has the same sign as the tree-level coupling, leading to a quite large total coupling. The branching ratio falls off quickly for smaller sfermion masses, since here $\sin\alpha$ becomes sizable (and positive). Moreover, for $m_{\tilde{l}} \simeq 210$ GeV the tree-level and one-loop contributions to the couplings have opposite sign. The branching ratio also decreases when $m_{\tilde{l}}$ is raised above 250 GeV, albeit somewhat more slowly; here the rapid decrease of the loop contribution is compensated by the increase of the tree-level coupling, which however does not suffice to compensate the simultaneous increase of $\sin^2\alpha$.

Fig. 4 shows the dependence of the $h\tilde{\chi}_1^0\tilde{\chi}_1^0$ coupling and of the corresponding h branching ratio on the mass of the LSP, $m_{\tilde{\chi}_1^0} \simeq M_1$. We see that the tree-level contribution to this coupling depends essentially linearly on the LSP mass. Eqs. (2) and (7) show that, for the given scenario where $c_\alpha \simeq s_\beta \simeq 1$, this linear dependence on M_1 originates from N_{14} , where

¹¹For the choice of parameters in Fig. 3 the total decay width of h is similar to, or even smaller than, that of the Standard Model Higgs boson with equal mass.

the contribution with M_1 in the numerator is enhanced by a factor of $\tan\beta$ relative to the contribution with μ in the numerator. Therefore the contribution $\propto M_1$ is not negligible even though in Fig. 4 we have $M_1 \ll |\mu|$. On the other hand, the one-loop contribution to this coupling depends only very weakly on M_1 . The small increase of this contribution shown in Fig. 4 is mostly due to the explicit $m_{\tilde{\chi}_1^0}$ dependence of the loop coupling (19); the change of N_{12} with increasing M_1 , as described by eq. (7), plays a less important role. The increase of the total coupling with increasing M_1 nevertheless remains significant. However, the right panel in Fig. 4 shows that for $m_{\tilde{\chi}_1^0} \gtrsim 15$ GeV this increase of the coupling is over-compensated by the decrease of the β^3 threshold factor in the expression (28) for the h partial width.

Once one-loop corrections are included, for certain values of the MSSM parameters the branching ratio for invisible h boson decays can thus reach the level of several percent even if $\tilde{\chi}_1^0$ is an almost purely bino. This would make the detection of these decays possible at the next generation of e^+e^- linear colliders. At such a collider it will be possible to isolate $e^+e^- \rightarrow Zh$ production followed by $Z \rightarrow \ell^+\ell^-$ decays ($\ell = e$ or μ) *independent* of the h decay mode, simply by studying the distribution of the mass recoiling against the $\ell^+\ell^-$ pair. This allows accurate measurements of the various h decay branching ratios, including the one for invisible decays, with an error that is essentially determined by the available statistics [22]. Since a collider operating at $\sqrt{s} \sim 300$ to 500 GeV should produce $\sim 10^5$ Zh pairs per year if $|\sin(\alpha - \beta)| \simeq 1$ one should be able to measure an invisible branching ratio of about 3% with a relative statistical uncertainty of about 2%.

We now turn to the heavier MSSM Higgs bosons H and A . The couplings to the lightest neutralinos are shown in Fig. 5 for the same input parameters as in Fig. 2. As can be seen, up to a relative minus sign, the tree-level couplings of these two Higgs bosons are approximately the same since we are in the decoupling regime where $d_A \simeq -d_H$, and $e_A \simeq e_H$ with $|e_A| \ll 1$, see eq. (4). Eqs. (2–4) and (7) also show that the tree-level couplings of the heavy Higgs bosons exceed that of the light Higgs boson h by a factor $\tan\beta/2$ [ignoring contributions to eqs. (7) with M_1 in the numerator]. On the other hand, the loop corrections are smaller in case of the heavy Higgs bosons. The corrections to the $H\tilde{\chi}_1^0\tilde{\chi}_1^0$ coupling are reduced by about a factor of 2 compared to the corrections to the $h\tilde{\chi}_1^0\tilde{\chi}_1^0$ coupling, mostly due to the relatively smaller coupling to \tilde{t}_1 pairs, see eqs. (22). The corrections to the $A\tilde{\chi}_1^0\tilde{\chi}_1^0$ coupling are even smaller, since the CP-odd Higgs boson A cannot couple to two identical squarks. The contribution with two \tilde{t}_1 squarks and one top quark in the loop, which dominates the corrections to the couplings of the CP-even Higgs bosons for small $m_{\tilde{t}}$, does therefore not exist in case of the A boson. As a result, the corrections to the coupling of A are not only smaller, but also depend less strongly on $m_{\tilde{t}}$; recall that for our choice of parameters $m_{\tilde{t}_1}$ increases very quickly as $m_{\tilde{t}}$ is increased from its lowest allowed value of ~ 210 GeV, which comes from the requirement $m_{\tilde{t}_1} \geq 100$ GeV. Note also that the Htt and Att couplings are suppressed by a factor $\cot\beta$ relative to the htt coupling, see eqs. (21); this becomes important for large squark masses, where the contributions from Fig. 1b are relatively less important. Altogether we thus see that the one-loop corrections are much less important for the heavy Higgs bosons. Note also that for the given set of parameters they tend to *reduce* the absolute size of these couplings.

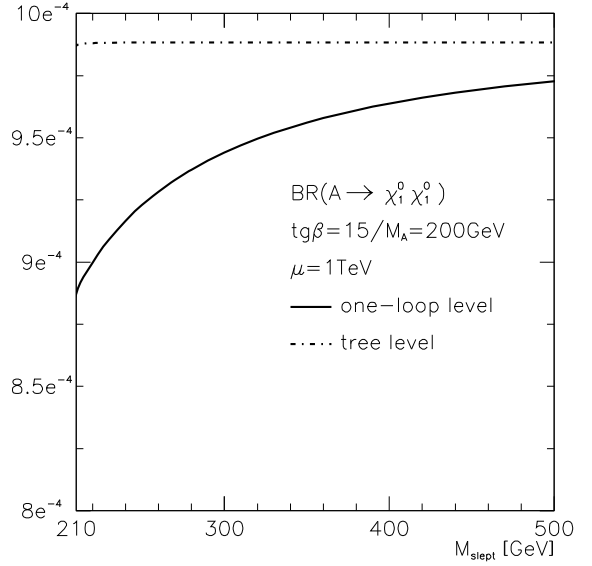
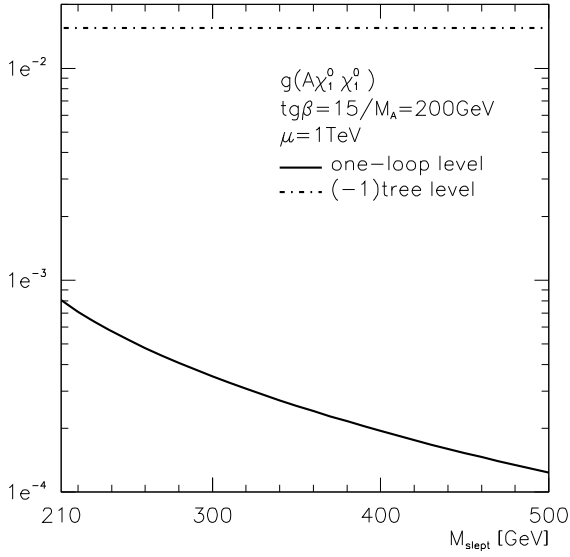
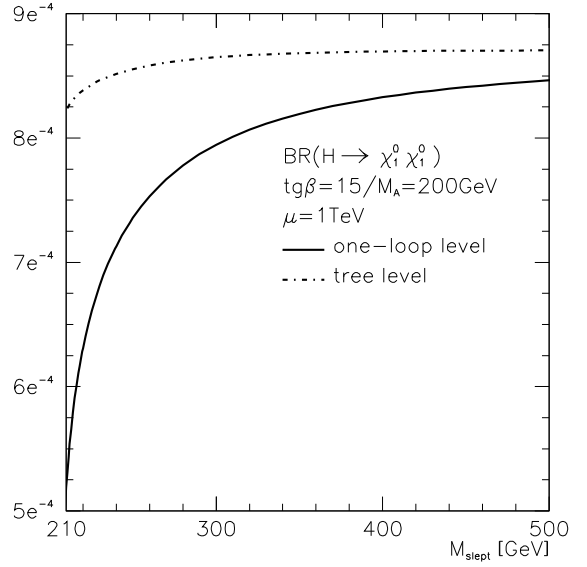
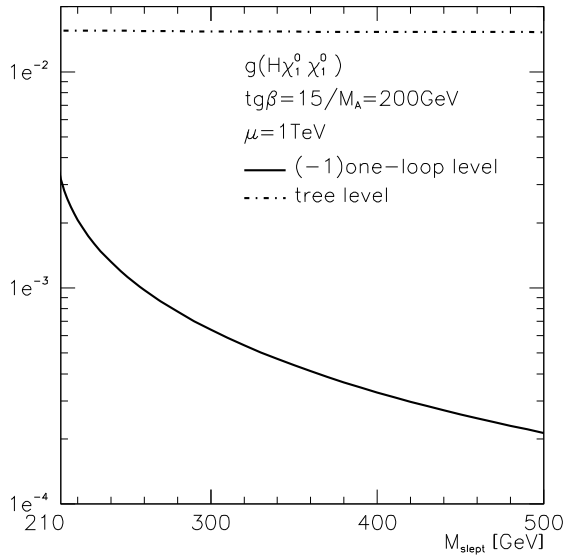


Figure 5: The heavier CP-even Higgs boson H (upper plots) and the pseudoscalar A boson (lower plots) couplings (left) and branching ratios (right) to pairs of the lightest neutralinos as functions of the common slepton mass. The parameters are as in Fig. 2.

The partial decay width $\Gamma(H \rightarrow \tilde{\chi}_1^0 \tilde{\chi}_1^0)$ of the CP-even Higgs boson H is given by eq. (28) with $\phi = H$. Due to the different CP nature of the pseudoscalar Higgs boson A , the expression for its partial decay width differs slightly; it is given by:

$$\Gamma(A \rightarrow \tilde{\chi}_1^0 \tilde{\chi}_1^0) = \frac{\beta_A M_A}{16\pi} \left| g_{A\tilde{\chi}_1^0 \tilde{\chi}_1^0}^0 + g_{A\tilde{\chi}_1^0 \tilde{\chi}_1^0}^1 \right|^2. \quad (29)$$

Again, because in the decoupling regime the CP-even H boson and the pseudoscalar A boson have almost the same couplings to Standard Model particles and to the neutralinos [at the tree level], their branching ratios are approximately the same. The one-loop contributions decrease the branching ratios by at most ~ 10 to 40%. Note that the total decay widths of the A and H bosons are strongly enhanced by $\tan^2 \beta$ factors [$\Gamma(H, A \rightarrow b\bar{b}) \propto m_b^2 g_{A,Hbb}^2$]. This over-compensates the increase of their couplings to neutralinos, so that their branching ratios into $\tilde{\chi}_1^0$ pairs are far smaller than that of the light Higgs boson h , remaining below the 1 permille level over the entire parameter range shown. Moreover, the cross section for the production of heavy Higgs bosons at e^+e^- colliders is dominated by associated HA production, which has a much less clean signature than Zh production does. Branching ratios of the size shown in Fig. 5 will therefore not be measurable at e^+e^- colliders. In fact, they will probably even be difficult to measure at a $\mu^+\mu^-$ collider “Higgs factory”; recall that the Z factories LEP and SLC “only” determined the invisible decay width of the Z boson to $\sim 0.1\%$, see eq. (27).

4 SUSY Dark Matter

It is well known that in the MSSM with exact R-parity, the lightest neutralino is a good cold Dark Matter (DM) candidate [2, 3]. For a very reasonable range of supersymmetric parameters the relic density of a bino-like neutralino satisfies $0.1 \lesssim \Omega_{\tilde{\chi}_1^0} h^2 \lesssim 0.3$, which is the currently preferred range [23]; here Ω denotes the mass density in units of the critical density, and h is today’s Hubble constant in units of 100 km/(sec·Mpc). Note that this argument singles out a bino-like LSP. A higgsino- or wino-like LSP would have a thermal relic density in this range only if its mass is around 1 TeV; such a large mass for the *lightest* superparticle would be difficult to reconcile with finetuning or naturalness arguments.

The two relic neutralino search strategies that suffer least from our lack of knowledge of the DM distribution throughout our galaxy are “direct” detection, where one looks for the elastic scattering of ambient neutralinos off nuclei in a detector; and the “indirect” search for high-energy neutrinos originating from $\tilde{\chi}_1^0 \tilde{\chi}_1^0$ annihilation in the center of the Earth or Sun. In both cases the signal rate is directly proportional to the LSP-nucleon cross section [3]. This cross section in turn depends on the neutralino-quark interaction strength, on the distribution of quarks in the nucleon, and on the distribution of nucleons in the nucleus.

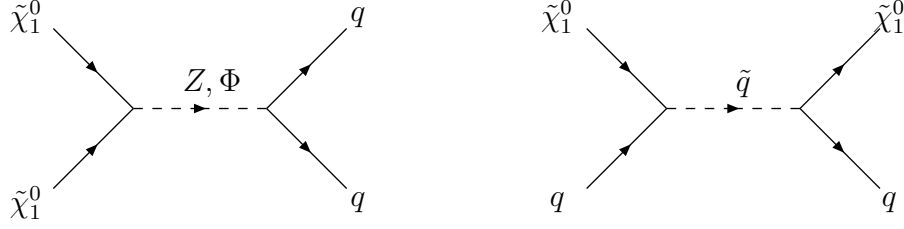


Figure 6: Diagrams contributing to the effective neutralino–quark interactions.

Three classes of diagrams contribute to the neutralino quark interaction: the exchange of a Z or Higgs boson in the t –channel, and squark exchange in the s – or u –channel, see Fig. 6. Z exchange only leads to a spin–dependent interaction, while Higgs exchange contributes only to the spin–independent interaction, and squark exchange gives both spin–dependent and spin–independent contributions, where the latter arises only due to combinations of couplings that violate chirality; see Ref. [3] for details. In general the spin–independent contribution is more important since it leads to a *coherent* coupling to heavy nuclei¹², and the Higgs exchange contribution is usually bigger than the squark exchange contribution.

We saw in Sec. 2.1 that in the pure gaugino limit the $\tilde{\chi}_1^0 \tilde{\chi}_1^0$ Higgs couplings vanish at the tree level. We just stated that the most important contribution to the spin–independent neutralino quark interaction often comes from Higgs exchange. In this Section we therefore study the effect of the fermion–sfermion loop corrections to the Higgs couplings to neutralinos on the neutralino–proton cross section. We use the expressions in Ref. [24]; these expressions also include contributions from effective LSP–gluon interactions. We also take into account leading SUSY QCD corrections to the scattering cross section [25], and assume the “standard” value [3] for the strange contribution to the nucleon mass, $m_s \langle p | \bar{s}s | p \rangle = 130$ MeV.

As in Sec. 2 we use non–universal soft breaking terms but keep all squark masses identical. All experimental constraints on sparticle and Higgs boson masses are taken into account. We show two illustrative examples. In Fig. 7 we take $m_{\tilde{\chi}_1^0} \simeq M_1 = 50$ GeV, and vary μ from 700 to 1050 GeV. The values of the other parameters are similar to those of Fig. 2. The upper panel shows the predicted relic LSP proton scattering cross section, while the lower panel shows the thermal LSP relic density $\Omega_{\tilde{\chi}_1^0} h^2$. In the case at hand this latter quantity is essentially determined [3] by $\tilde{\chi}_1^0$ pair annihilation into charged lepton pairs. The rapid decrease with increasing μ is due to the decrease of $m_{\tilde{\tau}_1}$, which is caused by enhanced $\tilde{\tau}_L - \tilde{\tau}_R$ mixing; this not only trivially increases the $\tilde{\tau}_1$ propagator, but also allows $\tilde{\chi}_1^0$ annihilation to proceed from an S–wave initial state [9]. We include this figure here in order to illustrate that our choice of parameters leads to an LSP relic density of the required magnitude. Of course, this is not difficult to arrange, since the loop corrections we are interested in

¹²The $\tilde{\chi}_1^0$ capture rate in the Sun, which contains very few heavy nuclei, can also get important contributions from spin–dependent interactions.

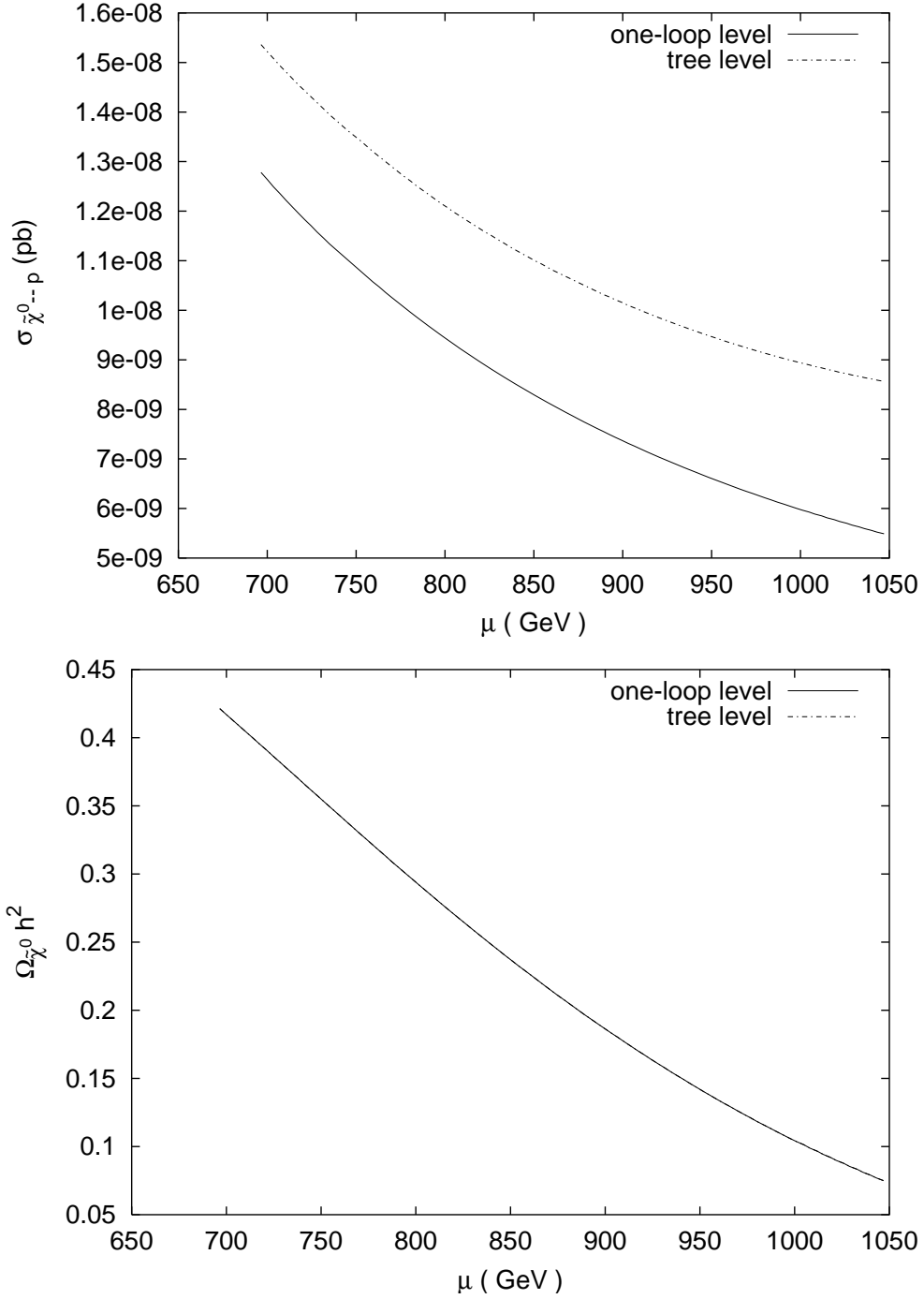


Figure 7: The predicted neutralino–proton scattering cross section and the thermal relic density (bottom), when one-loop corrections to the couplings of the Higgs boson to the LSP are included (solid curves) or omitted (dashed curves); in the lower frame the two curves practically lie on top of each other. The values of the relevant parameters are: $m_{\tilde{\chi}_1^0} \simeq M_1 = 50$ GeV, $m_{\tilde{q}} = 400$ GeV, $M_A = 200$ GeV, $M_2 = 105$ GeV, $A_q = 2.73m_{\tilde{q}}$, $\tan \beta = 21$, $m_{\tilde{e}_R} = 210$ GeV, and $m_{\tilde{\nu}} = 200$ GeV.

are almost independent of soft breaking parameters in the slepton sector, which therefore always can be chosen to produce the desired relic density, as long as the LSP is not too heavy. Not surprisingly, the prediction of $\Omega_{\tilde{\chi}_1^0} h^2$ is practically not affected by the loop corrections presented in Sec. 2.

On the other hand the effect of these corrections on the LSP–nucleon scattering cross section can be significant, as shown in the upper frame of Fig. 7, where they reduce the predicted scattering rate by up to a factor of 1.5. For the given choice of parameters the tree–level and one–loop contributions to the $h\tilde{\chi}_1^0\tilde{\chi}_1^0$ coupling have opposite sign, as in the upper frames of Fig. 3; the absolute value of the sum of these contributions only amounts to about 20% of the absolute value of the tree–level coupling. However, the scattering cross section is actually dominated by the exchange of the heavier H boson. For the given choice of parameters its mass exceeds M_h only by a factor of ~ 1.5 , and its couplings to down–type quarks are enhanced by a factor $\sim \tan\beta$; moreover, we saw in Sec. 3 that $|g_{H\tilde{\chi}_1^0\tilde{\chi}_1^0}^0|$ exceeds $|g_{h\tilde{\chi}_1^0\tilde{\chi}_1^0}^0|$ by a factor $\sim \tan\beta/2$. The absolute value of the $H\tilde{\chi}_1^0\tilde{\chi}_1^0$ coupling is also reduced here, as in Fig. 5, but only by $\sim 10\%$. Another significant contribution comes from \tilde{s} squark exchange, since $\tilde{s}_L - \tilde{s}_R$ mixing is enhanced for large $|\mu| \cdot \tan\beta$; this mixing increases the spin–independent part of the squark exchange contribution [27]. Of course this latter contribution, which interferes constructively with the H –exchange contribution, is not affected by the loop corrections of Sec. 2. Hence in the given case the net effect of these corrections is significantly smaller than in case of the invisible width of the h boson. Finally, the overall decline of the predicted LSP scattering rate with increasing μ is due to the reduction of the higgsino components of the LSP, see eqs. (7), which leads to smaller tree–level LSP couplings to the Higgs bosons. Since the one–loop corrections to the Higgs couplings depend only rather weakly on μ they become relatively more important when $|\mu|$ is increased.

As a second example, shown in Fig. 8, we take $m_{\tilde{\chi}_1^0} \simeq M_1 = 100$ GeV, and slightly reduced values for m_A and $\tan\beta$. The reduction of $\tan\beta$ implies less $\tilde{\tau}_L\tilde{\tau}_R$ mixing, so that the relic density is much less sensitive to μ than in the previous example. On the other hand, the increase of the LSP mass while keeping the slepton masses essentially the same leads to an increase of the annihilation cross section, so that we now obtain a relic density of the required size in the entire range of μ shown in this figure. The effect of the loop corrections to the Higgs $\tilde{\chi}_1^0\tilde{\chi}_1^0$ vertices is somewhat larger here than in the previous example. Due to the reduced value of M_A we are now in a regime with strong Higgs mixing, i.e. $|\sin\alpha|$ is much larger than the value $\cos\beta$ it takes in the limit $M_A \rightarrow \infty$. As a result the exchange of the lighter h boson is now more important than before. The loop corrections reduce the absolute value of the $h\tilde{\chi}_1^0\tilde{\chi}_1^0$ coupling by about a factor of two, which leads to a similar reduction of the predicted LSP scattering rate.

We already saw in Sec. 3.2 that loop corrections to the Higgs $\tilde{\chi}_1^0\tilde{\chi}_1^0$ couplings are maximal if \tilde{t}_1 is light and the Higgs $\tilde{t}_1\tilde{t}_1$ couplings are large. This is again illustrated in Fig. 9, where we show the dependence of $\sigma_{\tilde{\chi}_1^0\tilde{\chi}_1^0}$ on A_t (top) and $\tan\beta$ (bottom). Reducing A_t from its upper bound (set by the experimental lower bound on m_h) increases $m_{\tilde{t}_1}$ and reduces the $h\tilde{t}_1\tilde{t}_1$ coupling, which leads to a rapid decrease of the loop correction to $\sigma_{\tilde{\chi}_1^0\tilde{\chi}_1^0}$. The A_t

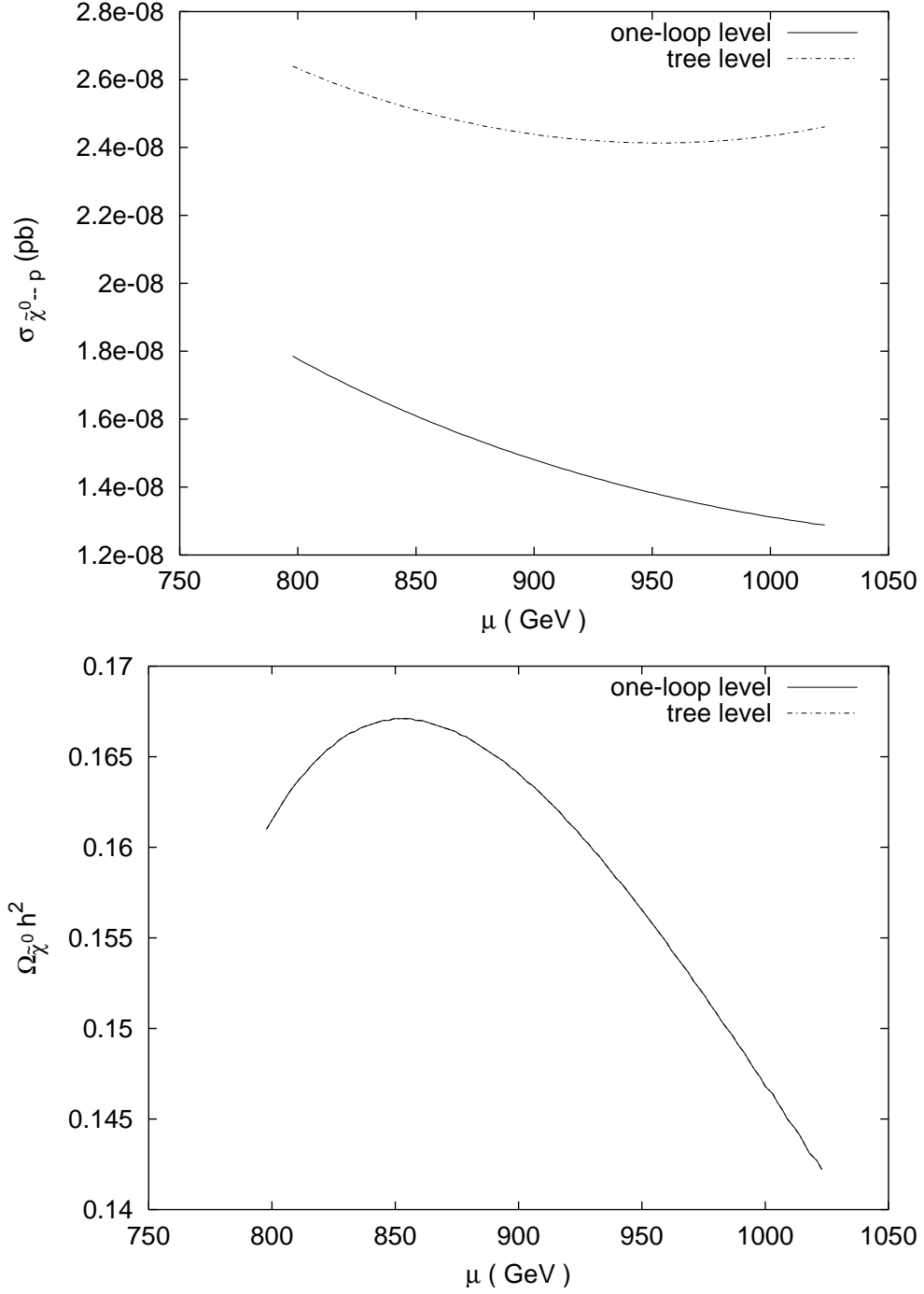


Figure 8: As in Figure 7, but for the following set of input parameters: $m_{\tilde{\chi}_1^0} = 100$ GeV, $m_{\tilde{q}} = 400$ GeV, $M_A = 150$ GeV, $M_2 = 200$ GeV, $A_q = 2.77m_{\tilde{q}}$, $\tan\beta = 14$, and $m_{\tilde{e}_R} = m_{\tilde{\nu}} = 200$ GeV.

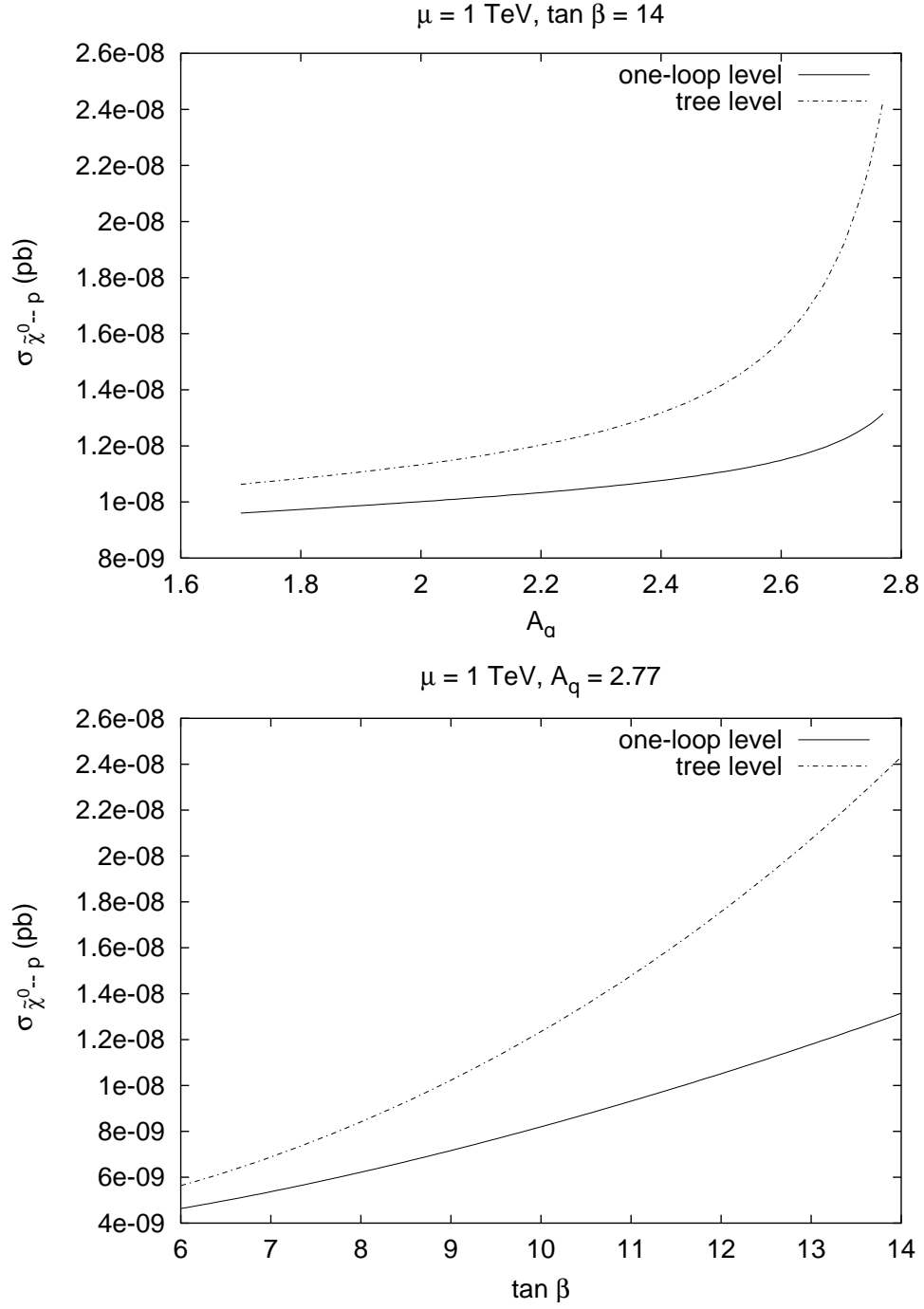


Figure 9: The dependence of the $\tilde{\chi}_1^0 - p$ cross section on A_t (top) and $\tan \beta$ (bottom) for $\mu = 1$ TeV. The values of the other parameters are as in Fig. 8. The upper bound on A_t and both the upper and lower bound on $\tan \beta$ are determined by the experimental lower bound on m_h .

dependence of the tree-level prediction is due to the $t - \tilde{t}$ loop corrections to the MSSM Higgs sector, which are always included. This dependence is quite mild, except near the upper bound on A_t where both m_h and the mixing angle α depend sensitively on A_t . On the other hand, the tree-level prediction for the scattering cross section depends quite strongly on $\tan \beta$, due to the $1/\cos \beta$ -behavior of the Yukawa couplings of down-type quarks. However, the negative loop corrections also increase in size with increasing $\tan \beta$, largely due to the $\tan \beta$ dependence of the Higgs couplings to t and \tilde{t}_1 (recall that we are far away from the “decoupling limit”). We thus see that in the case at hand the parameter dependence actually becomes weaker once loop corrections are included; however, this is not always the case. Finally, we note that scenarios with $m_{\tilde{t}_1} \sim m_h$, where our loop corrections will be sizable, can also be found [28] in models with universal soft breaking terms at the scale of Grand Unification, if the trilinear soft breaking parameter is sizable already at this scale; the condition $|\mu| \gg M_1$ is almost always satisfied in these models.

In these two examples the corrections to the Higgs couplings to the LSP reduce the predicted scattering rate. It is easy to construct scenarios with even larger but positive corrections, by taking very large values for first and second generation squark masses as well as for M_A , while keeping third generation squark masses relatively small; this kind of spectrum is e.g. expected in “more minimal” supersymmetric models [29]. The largest contribution to the LSP–nucleon scattering cross section then comes from h exchange, so the corrections to this cross section would scale essentially like the square of the correction to the $h\tilde{\chi}_1^0\tilde{\chi}_1^0$ coupling discussed in Sec. 2.2. However, the predicted counting rate in such a scenario would be very low, well below the sensitivity of near future experiments. We finally note that the corrections to the $Z\tilde{\chi}_1^0\tilde{\chi}_1^0$ couplings will have some effect on the spin-dependent LSP–nucleon scattering cross section. However, this cross section is usually dominated by first and second generation squark exchange, which in this case does not require violation of chirality. We therefore expect the loop corrections to the Z coupling to be significant only in scenarios where $|M_1| \ll |\mu| \lesssim m_{\tilde{u},\tilde{d},\tilde{s}}$ but some sfermion masses are significantly smaller than $|\mu|$.

It should be noted that currently the $\tilde{\chi}_1^0 p$ scattering cross section can only be predicted to within a factor of 2 or so even if the fundamental LSP–quark interactions were known exactly, the main uncertainty coming from the poorly known size of the strange matrix element $m_s \langle p | \bar{s}s | p \rangle$. For the cases considered in this paper, the loop corrections calculated here can therefore shift the cross section by at most one “theoretical standard deviation”. However, this theoretical uncertainty will presumably be reduced in future. We believe that the calculation presented here, together with the results of refs.[13] and [25], reduces the theoretical uncertainty of the prediction of the hard scattering cross section for given SUSY parameters to the level of 10%.

5 Summary and conclusions

In this paper we have studied quantum corrections to the couplings of the Z and neutral Higgs bosons to gaugino-like neutralinos in the MSSM. We focused on the phenomenologically

most interesting case of a bino-like lightest neutralino $\tilde{\chi}_1^0$ as LSP, but our analytical results of Sec. 2 are valid for a more general gaugino-like neutralino, irrespective of whether it is the LSP. We found that these corrections can completely dominate the tree-level contribution to the coupling of the lightest CP-even Higgs boson. The corrections to the couplings of the Z and heavy CP-even Higgs boson are somewhat less significant, but can still amount to about a factor of 2. Since the CP-odd Higgs boson cannot couple to two identical sfermions the corrections are suppressed in this case. In all cases the corrections can be significant only if some sfermion masses are considerably smaller than the supersymmetric higgsino mass $|\mu|$. Both (s)lepton and (s)top loop contributions to the Z coupling can be important, since the experimental bounds for $m_{\tilde{t}_1}$ and $m_{\tilde{l}}$ are still quite close to M_Z . The Higgs couplings receive their potentially largest corrections from loops involving third generation quarks and their superpartners; in the latter case the corrections are also quite sensitive to the size of the trilinear soft breaking parameter A_t [and A_b , if $\tan\beta \gg 1$].

Turning to applications of these calculations, we found that these corrections might change the predicted detection rate of Dark Matter LSPs by up to a factor of two even for scenarios where the rate is close to the sensitivity of the next round of direct Dark Matter detection experiments. The possible impact on the invisible width of the lightest CP-even Higgs boson h is even more dramatic: it could be enhanced to a level that should be easily measurable at future high-energy e^+e^- colliders, even if the LSP is an almost perfect bino. This would open a new window for testing the MSSM at the quantum level.

Acknowledgments

This work is supported in part by the Euro-GDR Supersymétrie and by the European Union under contract HPRN-CT-2000-00149. MD thanks the KIAS school of physics in Seoul, Korea for their hospitality during the completion of this work; he is partly supported by the Deutsche Forschungsgemeinschaft through the SFB 375. PFP thanks the ICTP, Trieste, for hospitality while this work was completed.

References

- [1] H. P. Nilles, Phys. Rep. 110 (1984) 1; I. Simonsen, hep-ph/9506369.
- [2] H. Goldberg, Phys. Rev. Lett. 50 (1983) 1419; J. Ellis, J. S. Hagelin, D. V. Nanopoulos, K. Olive and M. Srednicki, Nucl. Phys. B238 (1984) 453.
- [3] G. Jungman, M. Kamionkowski and K. Griest, Phys. Rep. 267 (1996) 195, hep-ph/9506380.
- [4] T. Falk, R. Madden, K.A. Olive and M. Srednicki, Phys. Lett. B326, 125 (1994).
- [5] H.E. Haber and G.L. Kane, Phys. Rep. 117 (1985) 75.
- [6] For a review on the Higgs sector of the MSSM, see e.g.: J. Gunion, H. Haber, G. Kane and S. Dawson, *The Higgs Hunter's Guide*, Addison–Wesley, Reading 1990.
- [7] J.F. Gunion and H.E. Haber, Nucl. Phys. B272 (1986) 1, and erratum hep-ph/9301205.
- [8] M.M. El Kheishen, A.A. Shafik and A.A. Aboshousha, Phys. Rev. D45 (1992) 4345; M. Guchait, Z. Phys. C57 (1993) 157, erratum ibid. C61 (1994) 178; J.L. Kneur and G. Moutaka, Phys. Rev. D59 (1999) 015005, hep-ph/9807336; S.Y. Choi, J. Kalinowski, G. Moortgat-Pick and P.M. Zerwas, hep-ph/0108117.
- [9] M. Drees and M. M. Nojiri, Phys. Rev. D 47 (1993) 376.
- [10] A. Djouadi, J. Kalinowski, P. Ohmann and P.M. Zerwas, Z. Phys. C74 (1997) 93, hep-ph/9605339; see also, P.M. Zerwas (ed.) et al., Report of the Higgs working group in the ECFA–DESY Workshop (1996), hep-ph/9605437.
- [11] J. Ellis, S. Kelley and D.V. Nanopoulos, Phys. Lett. B260 (1991) 131; U. Amaldi, W. de Boer and M. Fürstenau, Phys. Lett. B260 (1991) 447; P. Langacker and M. Luo, Phys. Rev. D44 (1991) 817; C. Giunti, C.W. Kim and U.W. Lee, Mod. Phys. Lett. A6 (1991) 1745.
- [12] G.F. Giudice and A. Pomarol, Phys. Lett. B372 (1996) 253, hep-ph/9512337.
- [13] M. Drees, M.M. Nojiri, D.P. Roy and Y. Yamada, Phys. Rev. D56 (1997) 276, hep-ph/9701219, and erratum: Phys. Rev. D64 (2001) 039901.
- [14] W. Siegel, Phys. Lett. B84 (1979) 193; D. M. Capper, D.R.T. Jones and P. van Nieuwenhuizen, Nucl. Phys. B167 (1980) 479.
- [15] G. 't Hooft and M. Veltman, Nucl. Phys. B44 (1972) 189; P. Breitenlohner and D. Maison, Commun. Math. Phys. 52 (1977) 11.
- [16] G. Passarino and M. Veltman, Nucl. Phys. B160 (1979) 151.
- [17] Particle Data Group (D.E. Groom et al.), Eur. Phys. J. C15 (2000) 1.

- [18] For a recent compilation of LEP2 results on SUSY particles, see the talk of S. Rosier-Lees at the LEPC meeting on Nov. 3, 2000, and the talk given by J.F. Grivaz, at the conference “SUSY and Higgs”, Orsay, March 2001.
- [19] M. Carena, S. Mrenna and C.E.M. Wagner, Phys. Rev. D62 (2000) 055008, hep-ph/9907422; M. Carena, S. Heinemeyer, C.E.M. Wagner and G. Weiglein, hep-ph/9912223.
- [20] Invisible decays of the MSSM Higgs bosons have been discussed in: J.F. Gunion et al., Int. J. Mod. Phys. A2 (1987) 957; J.F. Gunion and H. Haber, Nucl. Phys. B307 (1988) 445; A. Djouadi, J. Kalinowski and P.M. Zerwas, Phys. Lett. B376 (1996) 220, hep-ph/9603368 and Z. Phys. C57 (1993) 569.
- [21] A. Djouadi, J. Kalinowski and M. Spira, Comput. Phys. Commun. 108 (1998) 56, hep-ph/9704448.
- [22] E. Accomando et al., Phys. Rep. 299 (1998) 1, hep-ph/9705442; TESLA TDR part 3, D. Heuer, D. Miller, F. Richard and P.M. Zerwas (eds.) et al., Report DESY-01-011C, hep-ph/0106315.
- [23] See e.g. J.R. Primack, talk at the “4th International Symposium on Sources and Detection of Dark Matter in the Universe (DM2000)”, Marina del Rey, California, Feb. 2000, astro-ph/0007187.
- [24] M. Drees and M. M. Nojiri, Phys. Rev. D47 (1993) 4226, and D48 (1993) 3483.
- [25] A. Djouadi and M. Drees, Phys. Lett. B484 (2000) 183, hep-ph/0004205.
- [26] J. Engel, S. Pittel and P. Vogel, Int. J. Mod. Phys. E1, 1 (1992).
- [27] M. Srednicki and R. Watkins, Phys. Lett. B225 (1989) 140.
- [28] T. Kon and T. Nonaka, Phys. Lett. B319 (1993) 355, hep-ph/9309286.
- [29] A.G. Cohen, D.B. Kaplan and A.E. Nelson, Phys. Lett. B388 (1996) 588, hep-ph/9607394.